PROPERTIES OF

THE SILICON SURFACE BARRIER COUNTER

A Thesis

Presented to

The Faculty of Graduate Studies

at the University of Manitoba

In Candidacy for the Degree of

Master of Science

by

Zivojin Nikolic

1966

A B S T R A C T

Properties of the Silicon Surface Barrier Counter

by

Z. Nikolic

A number of silicon surface barrier counters were made from n-type material having a resistivity of 400 ohm cm and their properties investigated. The counters had good energy resolution and could stand high bias voltages. The best room temperature energy resolution with 5.5 MeV alpha particles was 14.2 keV. It was found that after exposure to light the counters (in darkness) had higher reverse currents and poorer energy resolution, but after being kept in darkness for one or two days they regained their original properties. The effect was reproducible. The collection efficiency of the counters was bias dependent. The resolution for alpha particles was not limited by noise; there was a discrepancy between the measured and the calculated values of resolution. The discrepancy was composed of two components; one of them decreased with bias and the other increased with bias. In the case of the best resolution counter at biases below 300 V only the first component was present. The logarithm of the discrepancy plotted against the charge collection efficiency gave a straight line with negative slope, indicating that one part of the pulse height spread may be due to carrier recombination in the plasma region. It is believed that the cause of the other component of discrepancy is some sort of carrier multiplication.

C O N T E N T S

Page

List of figures

Page

I N T R O D U C T I O N

The main purpose of the present work is to investigate the physical properties of the silicon surface barrier counter.

Much work has been done on semiconductor counters so far. Many papers have been published and several conferences held, some of them dealing with semiconductor counters exclusively. The work is still in progress, but the frontier of research in the field seems to have moved from the junction counters towards the germanium lithium ion drift counters which can have deeper sensitive regions and which are more suitable for beta and gamma ray spectroscopy.

However, many properties which are common for all varieties of semiconductor counters still are not well understood or explained. There are unknown factors which affect the counter properties and a consequence of that is uneven and irreproducible results. In the literature concerning applications of the counters it is often emphasized that semiconductor counters have high stability and reproducibility of properties. But this is only relatively true. Closer examination of the properties reveals irreproducibilities which are great obstacles in studying and understanding them.

The ultimate energy resolution for electrons and gamma rays is limited by noise, but for heavy particles, such as alpha particles, the resolution is poorer than would result

from the noise level. This means that there are causes other than noise and statistical fluctuations which determine the pulse height spread in the case of heavy particles. It seems that it is not quite clear what these factors are. A good deal of the present work is devoted to this matter.

The surface barrier counter is very suitable for studying general physical properties of semiconductor counters because its manufacturing procedure is the simplest of all and the possibility of introducing additional unknown factors (there is no heating, for example) is least.

This work is divided in two parts. In the first part the physical principles of operation of the surface barrier counter are given. In the second part the results of experimental investigations are presented and discussed.

1. PHYSICAL PRINCIPLES AND PROPERTIES OF THE SURFACE BARRIER COUNTER

1.1 General operating principles.

When an energetic charged particle or a photon enters a semiconductor it loses its energy in collisions with electrons in the lattice, lifting the electrons from the lower energy bands to the upper bands and creating holes in the lower ones. After a very short time of the order of 10^{-12} seconds, the electrons fall from the upper bands to the bottom of the conduction band and the holes come to the top of the valence band. In this way a certain number Δn_o of free electron-hole pairs, in excess of the equilibrium number corresponding to the temperature of the semiconductor, is generated. These free carriers tend to recombine with each other, their number decreasing with time exponentially:

$$\Delta n = \Delta n_o e^{-\frac{t}{\tau}} \qquad (1)$$

where τ is the carrier lifetime.

The operation of a semiconductor counter is based on collection of the charge carried by the liberated carriers. The collected charge, or the voltage pulse corresponding to it, represents the signal by which the incident radiation is detected.

The maximum energy transferred to an electron by a heavy charged particle of mass M and having a nonrelativistic velocity is

$$E_{max} = 4 \frac{m}{M} E \ , \ (M >> m)$$

where E is the energy of the incident particle and m the electron mass. For a 5.5 MeV alpha particle E_{max} of the secondary electrons is less than 3 keV. In the case of incident electrons or gamma rays this energy of the secondary electrons may be much higher. Such an energetic secondary electron, losing its energy, produces further lower energy electrons and holes, and so on. The end of this cascade process is reached when the last generation of secondary electrons has not sufficient energy to lift other electrons to the conduction band. These electrons, which are quite numerous, lose their energy to lattice vibrations. During the process a large number of optical phonons is produced too.

Because of the last two parts of the process, that is because of the thermal (or phonon) losses, the energy ε required to generate one electron-hole pair is higher than the energy gap of the semiconductor. W. van Roosbroeck[1] showed recently that almost complete analogy exists between

the energy loss in a semiconductor and the so called "crazy carpentry" model. Using both analytical and Monte Carlo methods to solve the crazy carpentry problem for semiconductors, W. van Roosbroeck concluded, besides other things which will be mentioned later, that the average energy spent per electron-hole pair, ε , should be independent of the type and energy of the incident particle. Previously this fact was established experimentally. The first value of ε for silicon was reported in 1953 by McKay and McAffee[2] to be 3.5 eV, which is about three times higher than the energy gap. Still, this energy for generating one electron-hole pair is very low, about ten times lower than in gases, which is a great potential advantage of semiconductors when they are used for radiation counters.

When the incident particle energy is E then the number of pairs produced is E/ε and the liberated charge will be

$$Q = e \frac{E}{\varepsilon} , \qquad (2)$$

That is, proportional to the particle energy, since ε is constant. Denoting by q the collected charge, the col-

lection efficiency will be

$$\eta = \frac{q}{Q} \tag{3}$$

If η also were independent of the energy of the incident particle, the size of the signal, which is represented by the collected charge, would be proportional to the energy of the particle. This is the case only when η is close to unity.

The collection of the charge produced in the counter is achieved by means of an electric field which separates the electron-hole pairs and sweeps them out of the field region in the opposite directions towards relevant electrodes.

Let us consider a rectangular piece of semiconductor, say silicon, to see how it works as a counter. It is represented in fig. 1 with the simplest circuit. We shall assume a general case in which the electric field intensity may be an arbitrary function of the distance between the electrodes. Consider the motion under the influence of the electric field of one out of N carriers created by the incident particle. The motion of one carrier may be thought of as producing a small pulse, the whole signal being the sum of all these small pulses. This moving carrier induces charge on the electrodes which is opposite in sign to the charge which already exists on them. When the carrier of

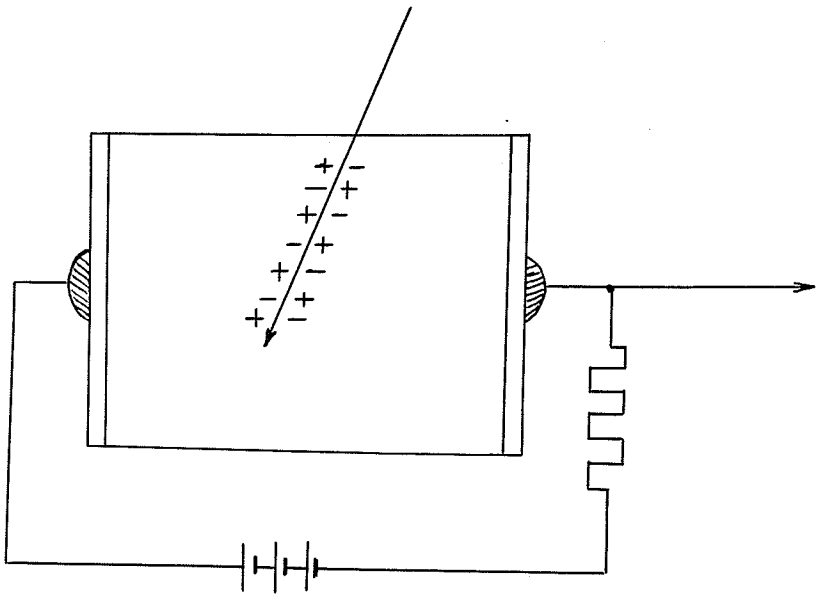

FIG. 1. SCHEMATIC DIAGRAM OF A SEMICONDUCTOR COUNTER.

charge e passes between the electrodes through a potential difference dU its energy increases by the amount edU, and this must be equal to the decrease Udq of the electrostatic energy of the system, which from the electrostatic point of view is represented by a capacitor, whose potential difference is U and charge is q. The induced charge on the electrodes (plates of the capacitor) is dq and it is actually a decrease of the charge which existed on the electrodes. So we have

$$edU = Udq \tag{4}$$

From equation (4) we get for the induced charge:

$$\Delta q_n = e \frac{\Delta U}{U}, \tag{5}$$

where ΔU is the potential difference crossed by the carrier inside the device. Quantity Δq_n is actually the collected charge on the electrodes due to the motion of one carrier, and it is seen that this is equal to one electronic charge only when ΔU equals the total voltage U across the device. Hence, only when both the electron and the hole belonging to a pair reach the electrodes, one electronic charge e is collected. The total charge collected Δq is the sum of all Δq_n.

As has already been mentioned the device is in fact a charged capacitor. The signal pulse due to the incident particle is formed in the following way: when the charge Δq created by the incident radiation is collected it decreases the charge q on the capacitor charged by means of the battery B to the potential difference U. The voltage across the capacitor drops because the battery, due to the presence of the load resistor R, can not replace immediately the charge on the capacitor which is being lost as a result of the motion of electron-hole pairs between its plates. This charge is replaced by the battery, that is the previous state is restored, with time constant $\theta = RC$, where C is the capacitance of the device. Thus, a voltage pulse of height

$$\Delta U = \frac{\Delta q}{C} \qquad (6)$$

is obtained. The rise time of the pulse on the counter alone is determined by the transit time of the carriers while the rise time at the input of the preamplifier is determined by the resistance of the base of the counter (undepleted region in the junction counter) and the capacitance of the input of the preamplifier together with stray capacitance.

Since the drift velocity of the carriers in the electric

field is μF, if μ is the mobility and F the electric field intensity, the carrier transit time is

$$t = \int_0^w \frac{dx}{\mu F(x)} \quad . \tag{7}$$

where w is the width of the depletion region. For densely ionizing particles the charge collection time is somewhat longer than the transit time of the slower carrier because some time elapses before the electric field penetrates the cloud of electrons and holes and separates them. Still, the slower carrier transit time is a realistic measure of the charge collection time and the rise time of the pulse. It should be mentioned, however, that the carrier mobility begins to decrease in high electric fields (above 10^3 V/cm). The pulse rise time in semiconductor counters is typically a few nanoseconds.

What has been said so far about the rise time applies to the case where all the charge carriers are generated in the region of high electric field. When some part of the particle track lies outside the field region, as is the case in p-n junction and surface barrier counters, when the particle range exceeds the depletion region width, the carriers may diffuse into this region and then be swept across it. In this case the time taken by the carriers to diffuse back to the end of the field region is approximately

$$t_D = \frac{x_D^2}{D} \tag{8}$$

where D is the diffusion constant and x_D the average distance that the carriers travel to the edge of the field region. Time t_D is of the order of microseconds, exceeding the transit time across the field region by two orders of magnitude. The two pulses, one due to the particle stopped in the depletion region and the other due to the particle penetrating it, are of different shape: the first one has a fast rise whereas the second has a long diffusion component added. Making use of this H.Funsten[3] designed a circuit for discrimination of these two pulses. This discrimination is useful in such experiments where peaks belonging to low energy particles stopped within the depletion region overlap the peaks of higher energy particles passing through.

From equation (5) it follows that, if the whole charge generated by the incident particle is to be collected, all the carriers must traverse the entire potential difference in the device. Recombination before collection must be prevented, and this can be achieved only if the collection time is much shorter than the carrier lifetime. Given the carrier lifetime and the distance w, the time t can be made shorter only be increasing the electric field intensity F (eq. 7). The most important point now is to realize a high electric field in the semiconductor without getting too high a current whose noise would contribute to the line

widths of the spectra obtained by the counter or even mask the signal. It would not be a great exaggeration to say that the whole problem of the semiconductor counter is to find a compromise between the two mutually opposite factors: high electric field necessary for good collection and low leakage current required for a low noise level, both in favor of good energy resolution.

This goal may be realized in two ways: first, by using a very high resistivity material, and second, by employing a p-n junction or a surface barrier diode. The first method resulted in the homogeneous conduction counter[4], while the second resulted in the so called junction counters to which belong the diffused p-n and n-p junction counter and the lithium ion drift counter. The junction counters are in fact reverse biased diodes whose space charge regions are the counter sensitive volumes. If a junction counter is to be a good energy spectrometer, the space charge region must lie immediately under the surface, and the width of the space charge region must exceed the incident radiation range. The lithium ion drift and the conduction counter, have the deepest sensitive regions so that they are suitable for beta and gamma spectrometry. The junction counters give the best results with heavy particles.

1.2 The surface barrier

It follows from the theory that in an ideal infinite crystal, where the lattice is perfectly periodic, there are no allowed energy levels for electrons in the energy gap between the conduction and the valence band. In a crystal of finite size the presence of the boundary already means that the periodicity is destroyed and it is not necessary that the above statement should hold in this case. In fact, Tamm[5] showed that in this case allowed electron energy levels in the forbidden energy gap could exist at the surface of the crystal, which correspond to the so called "surface states". Furthermore, there is an oxide layer on the crystal surface and over it a layer of adsorbed molecules from the surrounding atmosphere. The oxide layer and the adsorbed gases modify the surface energy levels and also introduce new surface states.

Consider an n-type semiconductor. When the surface states are filled with electrons the surface becomes negatively charged. Since the semiconductor must remain electrically neutral, a charge of the same magnitude as the surface charge but of the opposite sign is induced in a layer of the semiconductor underneath the surface. This layer of positive charge is in fact a space charge layer and it consists of positively charged donors. An electric

field exists in the space charge layer and there are no free carriers in it, so that it is often called the "depletion region". A potential difference across the depletion region, called the "built-in voltage", corresponds to the applied electric field. When suitable contacts are made on such a peice of semiconductor it will have rectifying properties, i.e. a diode is obtained. One of the contacts is usually a thin gold layer made by vacuum evaporation and this is the contact under which the space charge region is located. The other contact must be "ohmic" and it can be made in a number of different, more or less satisfactory, ways. Such a diode, biased in the reverse direction, is the surface barrier counter.

Since the diode space charge region is the sensitive region of the counter it will be of interest to find the width of this region and the electric field intensity in it as a function of the resistivity of the material used and the applied bias voltage. This can be done by solving the Poisson equation for this case, which represents the one dimensional case. The coordinate system (fig. 2) is place so that its origin is on the front surface and the x-axis perpendicular to it, that is, parallel to the electric field vector (but opposite in direction).

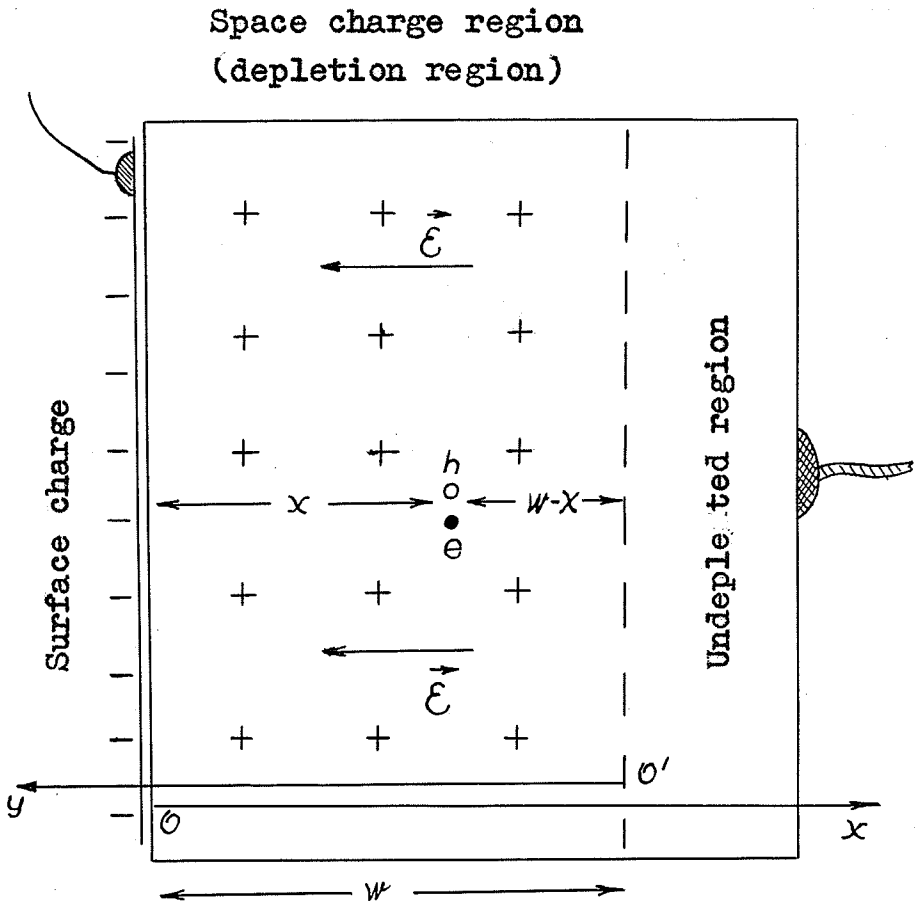

Fig. 2. Schematic diagram of the surface-barrier counter

If a voltage U_B is applied to the counter then the total voltage across it is $U = U_B + U_o$, where U_o is the built-in or intrinsic voltage. The Poisson equation in this case will be

$$\frac{d^2U}{dx^2} = -\frac{\delta}{\varepsilon} \quad , \tag{9}$$

where δ is the density of space charge in coul/m^3 and ε is the dielectric permittivity whose value for silicon is $12 \times \varepsilon_o$ ($\varepsilon_o = 8.85 \cdot 10^{-12}$ farad/meter). It will be assumed that the total voltage U across the device is given. The space charge density δ consists of the ionized donor concentration N_D which is constant throughout the volume, and free electron n_e and hole n_h concentrations.

$$\delta = e\left(N_D - n_e(x) + n_h(x)\right) \tag{10}$$

It would be very difficult to solve equation (9) taking for δ its value from (10). However, it will be a good approximation to take the free electron and hole concentrations equal to zero in the space charge region, that is to take

$$\delta = eN_D. \tag{10a}$$

for the room temperature conditions we are considering.

Integrating equation (9) and taking for boundary conditions that the electric field F is equal to zero at the inner boundary of the space charge region, x = w, where w is the width of the region (fig. 2), we get:

$$F = \frac{\delta}{\varepsilon} (x - w) \qquad (11)$$

Hence, the electric field intensity F is not constant. Its magnitude is greatest at the surface for x = 0, where it has the value

$$F_m = - \frac{\delta}{\varepsilon} w \ , \qquad (12)$$

and then falls off linearly with distance inside the space charge region. However, the lines of force of the electric field are parallel to each other and normal to the front surface.

The expression in parenthesis (x - w), in equation (11) is negative inside the depletion region (x < w), which means that the electric field vector is directed opposite to the x-axis.

Integration of equation (11), because $- \int_0^x F dx = U$, gives the potential difference U between the front surface and a point at x:

$$U = \frac{\delta}{2\varepsilon} [w^2 - (s - w)^2] \ . \qquad (13)$$

The total voltage across the depletion region (applied + intrinsic), U , is obtained for $x = w$:

$$U = \frac{\delta}{2\varepsilon} w^2 \quad . \tag{14}$$

Simpler relations for F and U are obtained if we place $x - w = y$. This is equivalent to using $O'y$ as a coordinate axis instead of Ox (fig. 2). Then we have:

$$F = \frac{\delta}{\varepsilon} y \quad ; \tag{11a}$$

and

$$U_y = \frac{\delta}{2\varepsilon} (w^2 - y^2), \tag{13a}$$

$$U = \frac{\delta}{2\varepsilon} w^2 \quad . \tag{14a}$$

From equation (14) it follows:

$$\frac{\delta}{\varepsilon} = \frac{2U}{w^2} \quad . \tag{15}$$

Making use of equation (15) equations (11a), (13a) and (11) may be rewritten in more useful forms for practical purposes:

$$F = \frac{2U}{w^2} y \quad ; \tag{11b}$$

$$U_y = \frac{U}{w^2} y^2 \quad ; \tag{13b}$$

$$F = \frac{2U}{w^2} (x - w) \quad . \tag{11c}$$

The magnitude of the largest and average values of electric field intensity are respectively

$$F_m = \frac{2U}{w} \tag{16a}$$

and

$$F_{av} = \frac{U}{w} \quad . \tag{16b}$$

From equation (14) the width of the space charge region may be expressed as a function of U:

$$w = \left(\frac{2\varepsilon U}{\delta}\right)^{\frac{1}{2}} \tag{17}$$

The density of the space charge δ is determined by the donor density N_D: $\delta = eN_D$, so that we have:

$$w = \left(\frac{2\varepsilon U}{eN_D}\right)^{\frac{1}{2}} \tag{18}$$

A semiconductor is usually characterized by resistivity ρ rather than by the impurity density. Instead of the donor density N_D we can introduce in the formula (18) the resistivity ρ as a parameter by means of the relation: $\rho = 1/eN_D\mu$, where μ is the carrier mobility, the mobility of electrons in this case. We have

$$w = (2\varepsilon\mu\delta U)^{\frac{1}{2}} \quad , \tag{19}$$

or, since ε and μ are constants for a given type of semiconductor, in the case of n-type silicon,

$$w = 0.536\ (\rho U)^{\frac{1}{2}} \text{ microns} \tag{20}$$

where ρ should be expressed in ohm·cm.

Hence, the width of the space charge region, the sensitive region of the counter, may be varied by varying the applied bias voltage. If one wants wider sensitive regions one has to make counters using low donor concentrations and apply high bias voltages.

The achievable depletion region widths range from a few microns to about 3 millimeters. Deepest barriers were achieved by R. J. Fox and C. J. Borkowski[6] and by E. D. Klema[7]. The last author obtained 3.5 mm deep sensitive regions using 20,000 ohm cm material with 1800 volts reverse bias.

From equations (16b) and (19) a relation between F_{av} and ρ and U may be obtained:

$$F_{av} \approx \frac{W}{\rho} , \tag{21}$$

and

$$F_{av} \approx \frac{U}{\rho}^{\frac{1}{2}} \tag{22}$$

The last two equations show that counters made of higher resistivity material have weaker electric fields.

The absolute value of the electric field intensity at the end of a 5.5 MeV alpha-particle track (range 26 microns) as a function of w and U for 400 ohm·cm n-type silicon is derived from equations (11) and (19):

$$F_R = 0.174(w - 26)\,kV/cm; \tag{23}$$

$$F_R = 1.87\ (U^{\frac{1}{2}} - 4.53)\ kV/cm, \tag{24}$$

where w is expressed in microns and U in volts. The last two equations are represented graphically in fig. 3 and fig. 4.

1.3 The counter capacitance.

A very important parameter of a counter is its capacitance. The size of the primary signal as well as the pulse risetime and the counter noise depend on this parameter.

It is often stated in the literature [8,9] that the capacitance of a p-n junction or surface barrier counter is the same as that of a parallel plate condenser. It should be pointed out that the two cases are not identical with respect to capacitance, though the dynamic capacitance of a barrier layer is the same as that of the parallel plate condenser of the same area and the same spacing between the plates. But this is merely a coincidence, because the field of the condenser is constant with respect to distance and the potential linear, while in a junction counter the electric field changes linearly with distance and potential is parabolic.

FIG. 3. ELECTRIC FIELD INTENSITY AT THE END OF 5.5 MeV ALPHA PARTICLE TRACK IN A 400 OHM·CM SURFACE BARRIER COUNTER AS A FUNCTION OF THE DEPLETION REGION WIDTH w.

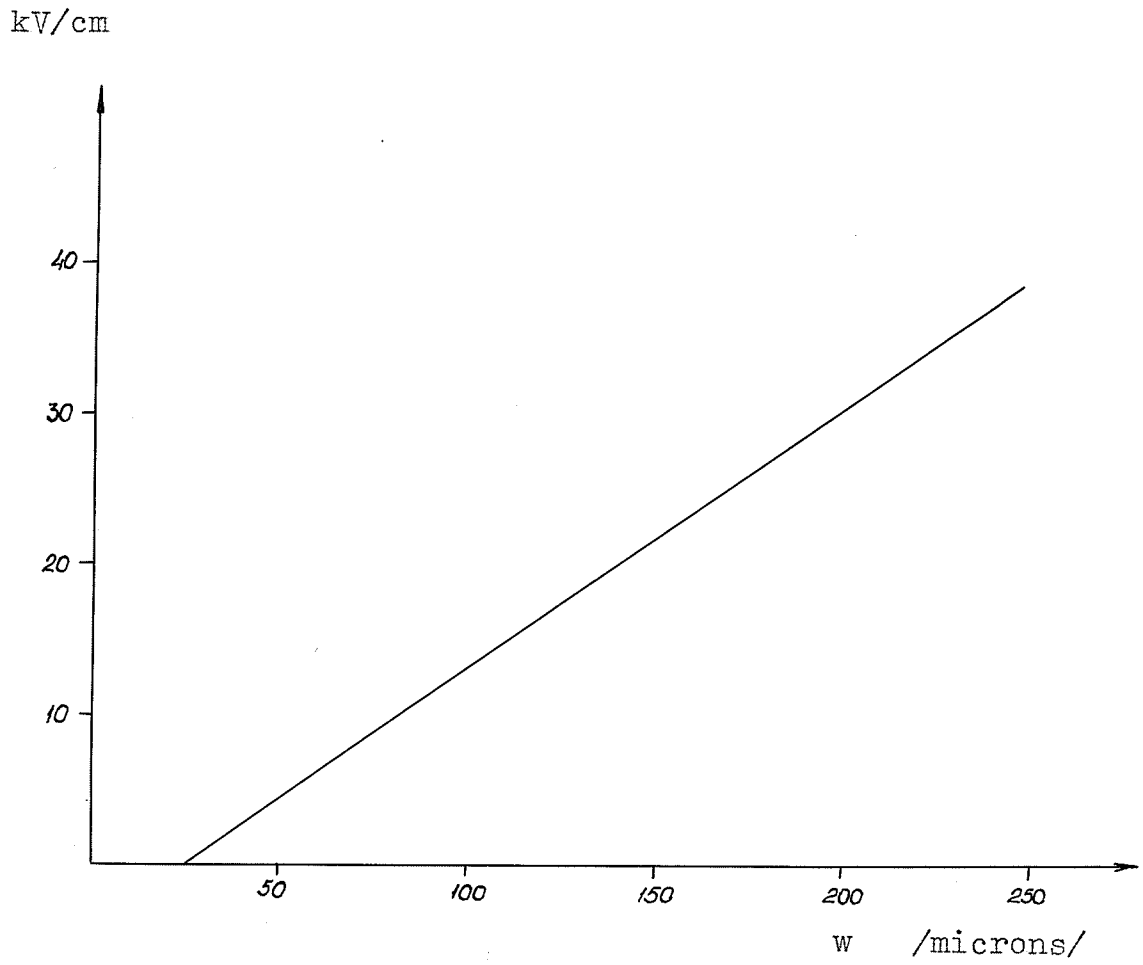

FIG. 4. ELECTRIC FIELD INTENSITY AT THE END OF 5.5 MeV ALPHA PARTICLE TRACK IN A 400 OHM·CM SURFACE BARRIER COUNTER AS A FUNCTION OF THE REVERSE BIAS VOLTAGE.

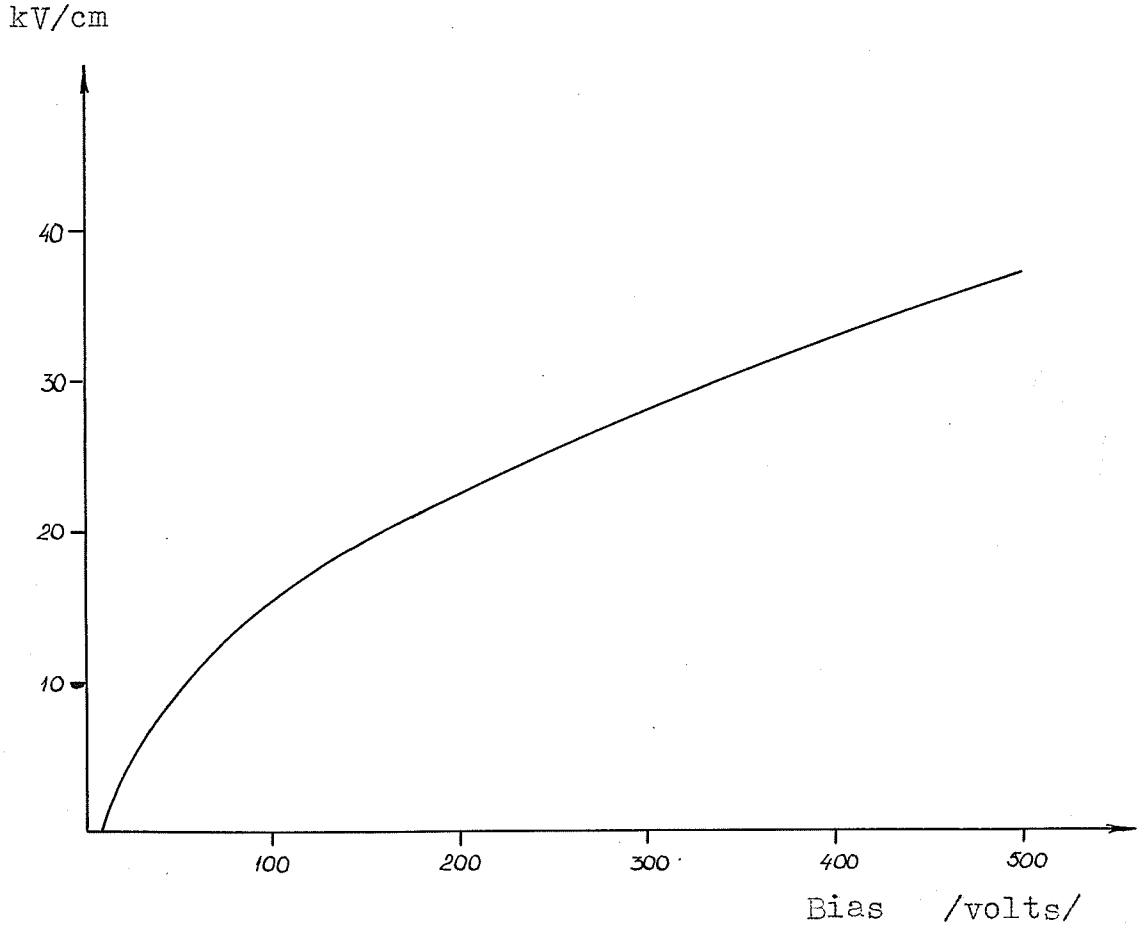

The static capacitance of the surface barrier counter is

$$C_{st} = \frac{Q}{U} = \frac{\delta w A}{\delta w^2/2\varepsilon} = \frac{2\varepsilon A}{w} \qquad (25)$$

where U is taken from equation (17) and A is the area.

The dynamic capacitance is

$$C_{dyn} = \frac{dQ}{dU} = \frac{\delta A\ dw}{(\delta w/\varepsilon)\ dw} = \frac{\varepsilon A}{w} \quad . \qquad (26)$$

Hence, the dynamic capacitance of the surface barrier is equal to the capacitance of a parallel plate condenser of the same area and silicon as dielectric, while the static capacitance is twice as large.

The dynamic capacitance determines the size of the primary signal and noise, but the static capacitance is the one determining the time constant.

The counter capacitance is bias dependent, because w varies with bias. Typical values of counter capacitance lie between 0.1 pF/mm^2 to about 15 pF/mm^2. The capacitance of a counter can be measured either by ordinary AC bridge methods[10] or by a method described by Dearnaley and Northrop[8], which consists of putting a condenser of known capacitance in parallel with the counter and comparing the pulse height in this case with the pulse height without the condenser (a voltage sensitive preamplifier is used).

Measurement of the capacitance supplies information about the width of the sensitive region and the resistivity of the material.

1.4 The reverse current.

When a reverse bias voltage is applied to the counter, a current flows through it which is called the reverse or leakage current.

The reverse current is composed of two main components: the bulk leakage current and the surface leakage current. The former consists of two parts, diffusion current and space charge generated current. Both of these current contributions are due to the existence of recombination centers[8,9]. A recombination center is an energy level in the forbidden energy gap, and it always acts so as to restore the equilibrium number of current carriers, when the equilibrium is disturbed.

A recombination center may assist recombination as well as act as a generation center. If the number of carriers is higher than the equilibrium number, recombination centers assist recombination; if lower they act as generation centers.

a. Diffusion current.

In the undepleted part of the surface barrier counter there is a certain concentration of free electrons and holes. When the holes, by diffusion, come to the edge of the depletion region where a strong electric field exists, they are swept across immediately, giving rise to the diffusion current. The current depends on the number of carriers (holes) arriving per unit time at the inner boundary of the field region. This number is[9]

$$= n_h l/\tau \ , \qquad (26)$$

where n_h is the hole concentration, l the distance from which they can diffuse to the boundary of the space charge region and τ the lifetime. The maximum value of l is equal to the diffusion length L when the undepleted region is thick. The diffusion current density is then

$$I_D = e n_h l/\tau \ . \qquad (27)$$

The hole concentration may be calculated from the "n-p" product:

$$n_e \cdot n_h = n_i^2 \ , \qquad n_h = n_i^2/n_e \ ,$$

(n_i is the intrinsic carrier concentration), but

the relation $\rho = 1/en_e\mu_e$ yields

$$1/n_e = \rho e\mu_e \quad ,$$

so that we have:

$$n_h = n_i^2 \rho e\mu_e \quad .$$

Intrinsic carrier concentration n_i is a constant for a given temperature, having the value $1.5 \times 10^{10} cm^{-3}$ at room temperature. Now equation (27) may be rewritten:

$$I_D = e^2 n_i^2 \mu_e \ell/\tau \qquad (28)$$

Taking for μ_e the value of 1350 $cm^2/V.sec$ and expressing τ in microseconds, we get

$$I_D = 7.7 \frac{\rho \ell}{\tau} 10^{-9} \text{ amp/cm}^2. \qquad (28a)$$

When $l = L$ and because $L = \sqrt{D_h \tau}$ it may be written:

$$I_D = 7.7 \times 10^{-9} \rho \sqrt{D/\tau} \qquad (29)$$

From the above consideration it may be concluded that the diffusion current is higher in devices made of higher resistivity material, because of higher hole concentration, and that longer carrier lifetime reduces it. When the thickness of the undepleted region is greater than L then the diffusion current is independent of the bias voltage.

For our counters made of 400 ohm·cm n-type silicon, if a lifetime of 10 microseconds is assumed, formula (29) gives: $I_D = 3.1 \times 10^{-9}$amp/cm^2.(In formula (29) D and τ should be expressed in CGS units and ρ in ohm·cm).

b. Space charge generated current.

There are no free carriers in the depletion region except those which are being generated in the region by the generating action of the recombination centers and which are swept across it immediately.

The generation rate g depends on the capture cross section for electrons and holes and location in energy of the recombination centers. These quantities are rarely well known, and in order to get some idea about the magnitude of the space charge generated current, the most unfavorable case will be assumed, when the recombination centers lie in the middle of the forbidden energy gap. The generation rate then has its maximum value[9].

$$g_{max} = n_i/2\tau \ , \qquad (30)$$

where n_i is the intrinsic electron concentration and τ the carrier lifetime.

Since the number of carriers generated in unit time per unit area of the counter is $g \cdot w$, the density of the space charge generated current, I_{sc}, will be

$$I_{sc} = gew \quad . \tag{31}$$

Because the width of the space charge region, w, is given by equation (19), I_{sc} is proportional to the square root of the bias voltage U.

In the worst case when the recombination centers lie in the middle of the energy gap, the space charge generated current is

$$I_{sc} = \frac{n_i e}{2\tau} w \quad . \tag{32}$$

In the case of our counters at 100 volts reverse bias $I_{sc} = 1.4 \cdot 10^{-6}$ amp/cm^2.

In practice the total reverse current of a counter often exceeds the sum of the diffusion and the space charge generated currents by about one or even two orders of magnitude. Besides this, the real reverse current is an irreproducible quantity, since it may differ in the case of two similar counters by as much as an order of magnitude. Both the diffusion current and the space charge generated current are completely determined by the characteristics of the material. Therefore, it must be concluded that the dominant part of the reverse current ought to be surface leakage current.

1.5 Charge collection and pulse formation.

The general principles of charge collection were discussed in secion 1.1. Now the problem of charge collection and pulse formation for the special case of surface barrier counters will be treated in more detail.

Again, for simplicity, motion of only one electron and one hole which originally belonged to the same pair will be considered. We shall find the time dependence of the collected charge referring to fig. 2 (page 15).

First, consider the electron contribution to the pulse. From the general expression (5)

$$\left(\Delta q_{ne}\right) = e \frac{\Delta U}{U} \qquad (33)$$

the time dependence of $\left(\Delta q_{ne}\right)$ may be found if the time dependence of the potential difference, U, crossed by the carrier is known. The latter will be known if the carrier position as a function of time is known.

Let $y = y(t)$ be the distance of the electron from the back boundary of the depletion region and let the pair be produced at time $t = 0$ at a distance $y = y_o$, then

$$\frac{dy}{dt} = - F(y)\mu_e \quad , \tag{34}$$

and from equation (11b)

$$\frac{dy}{dt} = - \frac{2U}{w^2} \mu_e y \ .$$

The negative sign occurs because the direction of the velocity is opposite to $\vec{F}$. Integration gives

$$y = y_o \, e^{- \frac{2U\mu_e}{w^2} t} \ . \tag{35}$$

Equation (35) indicates that the distance of the electron from the back boundary ($y = 0$) decreases exponentially with t and, is collected after an infinite time.

Using (13b) for ΔU in (33),

$$\Delta U = \frac{U}{w^2} \left(y_o^2 - y^2 \right) \quad , \tag{36}$$

where y is determined by equation (35). Therefore,

$$\left(\Delta q_{ne}\right) = e \, \frac{\Delta U}{U} = \frac{e \, U}{w^2 U} \, y_o^2 \left(1 - \exp\left[- \frac{4U\mu}{w^2} \, t \right] \right)$$

and

$$(\Delta q_{ne}) = e \frac{y_o^2}{w^2} \left(1 - \exp\left[-\frac{4u\mu_e}{w^2} t\right]\right) \qquad (37)$$

Taking $t \to \infty$ the total charge due to the electron is obtained:

$$(\Delta q_{ne}) = e \frac{y_o^2}{w^2} \quad . \qquad (38)$$

A similar procedure may be carried out for the motion of the hole:

$$\frac{dy}{dt} = F(y)\mu_h$$

$$\frac{dy}{dt} = \frac{2U}{w^2} \mu_h y \ , \qquad (39)$$

and

$$y = y_o e^{\frac{2U\mu_n}{w^2} t} \qquad (40)$$

From here, the time taken by the hole to cross from y_o to y is:

$$t_h = \frac{w^2}{2U\mu_h} \ln \frac{y}{y_o} \ , \qquad (41)$$

or, the total collection time,

$$T_h = \frac{w^2}{2U\mu_h} \ln \frac{w}{y_o} \quad . \qquad (42)$$

Combining equations (33), (36), and (40), charge

collected due to the motion of the hole is obtained:

$$\left(\Delta q_n\right) = e \frac{y_o^2}{w^2}\left(\exp\left[\frac{4U\mu_h}{w^2} t\right] - 1\right) \qquad (43)$$

Substituting in equation (43) for t with T_h given by expression (42), we have for the total charge due to the hole

$$\left(\Delta q_n\right)_{h,T} = e\left(1 - \frac{y_o^2}{w^2}\right) \qquad (44)$$

Summing the charges (38) and (44), the total charge due to the collection of both the electron and the hole of the original pair is found to be

$$\left(\Delta q_n\right)_{e,\ T} + \left(\Delta q_n\right)_{h,T} = e\ , \qquad (45)$$

as we already knew that it should be.

The charge pulse due to the incident particle is the sum of the pulses of all single electrons and holes generated by the incident particle.

It should be noted that the charge induced on the electrodes due to the motion of the hole is a positive exponential of time, while that due to the electron is a negative exponential. In addition to this, the electrons have to make on average longer trips than the holes. Therefore, it seems that the hole should be collected much faster

than the electron. But, as we shall see, this is not so.

The time constant of the electron collection process is

$$\theta = \frac{w^2}{4U\mu_e} \quad . \tag{46}$$

According to equation (19), $w^2 = 2\varepsilon\mu_e\rho U$, it follows that θ is independent of bias U and even independent of the carrier mobility:

$$\theta = \frac{2\varepsilon\mu_e\rho u}{4U\mu_e} = \frac{\varepsilon\rho}{2} \quad . \tag{47}$$

Again, consider our counters as an example. The time constant computed from equation (47) is $\theta = 2.1\text{x}10^{-10}$ second; 99.9% of the charge due to the electrons is collected after the time $t = 7\theta \approx 1.5$ nanoseconds.

The electron collection time is apparently independent of the initial position of the electron.

Combining equations (42) and (19), for the hole collection time we get:

$$T_h = \varepsilon\frac{\mu_e}{\mu_h}\rho \ln\frac{w}{y_o} \tag{48}$$

Since the hole collection time is dependent on the hole initial position y_o, we shall, as an example,

calculate the time for a hole which is generated in the middle of the depletion region, $y_o = w/2$:

$$T_h = \varepsilon \frac{\mu_e}{\mu_h} \rho \ln 2 = 0.83 \text{ n sec}$$

hence, it is not much shorter than the electron collection time. For $w/y_o = 10$ we have $T_h = 2.8$ n sec.

In practice, measured pulse risetimes are longer than the above calculated values. There are two reasons for that. First, the pulse risetime is made longer by the counter base resistance in conjunction with its capacitance. Second, it takes some time before the plasma in the initial ionization track is eroded away. Measured pulse risetimes reported in the literature are between a few nanoseconds and 10 nanoseconds [11, 12].

The above considerations are valid only when there is no trapping or recombination, i.e. all the carriers reach the boundaries of the space charge region. This is really the case in all practical surface barrier or p-n junction counters. For 99.9% collection efficiency it is sufficient that the collection time be 10θ or greater. This condition is satisfied when $\tau \geq 10$ μsec.

1.6 The energy resolution.

1.6.1 Introduction. A counter will never give exactly the same pulse height as a response to the same incident particle energy. The spectrum of pulse amplitudes due to a number of particles of the same energy will never be an infinitely narrow line but always a peak of a finite width. The width of the peak is a measure of the quality of the counter when it is used as an energy spectrometer, since this width determines the uncertainty with which the energy can be determined.

The full width of the peak at the half of its maximum height, expressed in units of energy or as a ratio to the peak position, is called the energy resolution of a counter. Resolution expressed in this way is usually designated as "FWHM" (Full Width at Half Maximum). The smaller FWHM the better a counter as an energy spectrometer.

When the pulse height distribution is Gaussian, it is more convenient for theoretical purposes to define resolution as the standard deviation of the distribution, δ. There is the following relation between the two ways of expressing resolution:

$$\text{FWHM} = 2.35 \times \delta \ .$$

There are several causes for the spread in the pulse height distribution. Some is due to noise of the associated electronics and drift in the amplifier and the pulse height analyzer, and they will not be treated here. The other factors which will be dealt with here are due to the counter itself. These are: the counter noise, the statistical fluctuations in the number of the electron-hole pairs and incomplete charge collection.

When the spread of the pulse height distribution is composed of a number of independent contributions, the FWHM is equal to the square root of the sum of squares of all contributions, or

$$[\Delta E]^2 = [\Delta E]_1^2 + [\Delta E]_2^2 + \ldots + [\Delta E]_n^2 \qquad (49)$$

where $[\Delta E]$ is the FWHM of the peak and $[\Delta E]_i$ separate contributions to the resolution.

1.6.2 The counter noise.

There is a natural limit in accuracy in the measurement of any quantity set by statistical fluctuations in the measuring device. These fluctuations are called noise. In a semiconductor counter only electrical noise is present, which consists of a fluctuating voltage. In this case noise

comes from two origins, so that there are two kinds: the thermal or Johnson noise and the current noise.

The noise pulses are superimposed on the signal pulses, causing a spread in their amplitudes. The magnitude of the spread depends on the noise level. The r.m.s. noise voltage is equal to the standard deviation ΔE_δ of the spread, if there is no other contribution to the spread.

a. Thermal noise.

In a resistor whose temperature is above absolute zero the current carriers move randomly in all direction, having a velocity distribution determined by the laws of statistical mechanics. These random carrier movements cause fluctuations of the charge to occur in the conductor, as a consequence of which a fluctuating voltage appears between the ends of the conductor. This voltage has components of all frequencies whose average value is zero but the r.m.s. value is finite.

We shall compute the mean square value of the noise making use of the law of equipartition of energy. The equivalent circuit which is assumed in the calculations is shown in fig. 5, where R_L is the load resistor, C_c and R_c

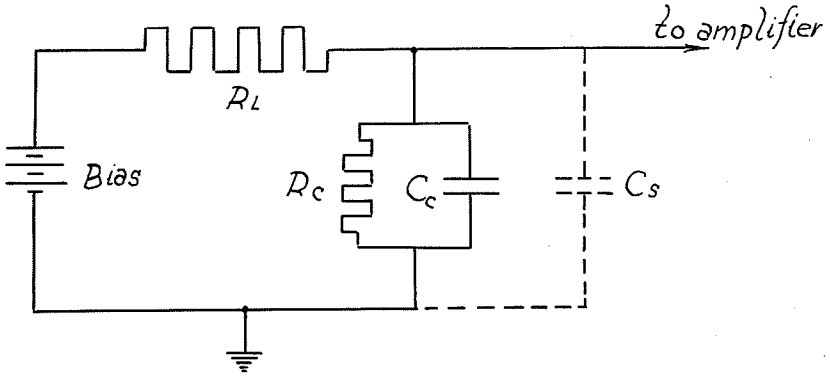

Fig. 5A

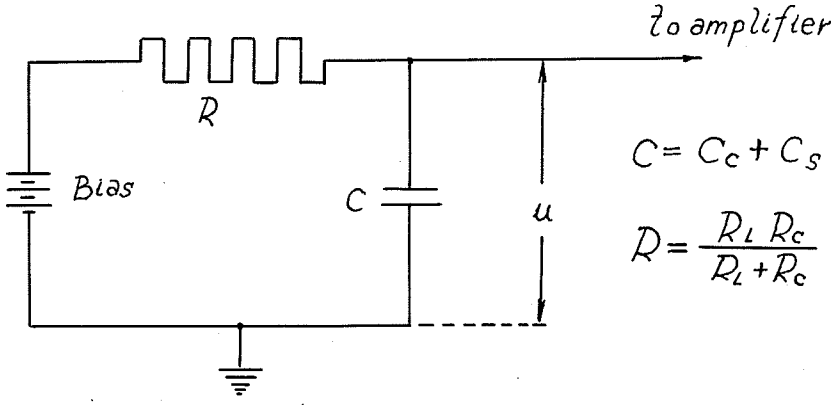

Fig. 5B

FIG. 5. EQUIVALENT CIRCUIT OF A SURFACE BARRIER COUNTER.

the counter capacitance and resistance respectively, and C_s the stray capacitance of the circuit including the input capacitance of the preamplifier. $C = C_c + C_s$, $R = R_L R_C / R_L + R_C$.

Voltage fluctuations on the resistance will induce charge and voltage fluctuation on the capacitance C and vice versa. The voltage fluctuations u on the capacitance, assuming that the circuit is in thermal equilibrium with the surroundings at the absolute temperature T, may be found by making use of the law of equipartition of energy and taking into account that the capacitance has one degree of freedom. The average potential energy on the capacitance is $\frac{1}{2}Cu^2$, and it ought to be

$$\frac{1}{2} C \bar{u}^2 = \frac{1}{2} k T \quad ,$$

which gives for the mean square noise voltage

$$\bar{u}^2 = \frac{k T}{C} \quad , \tag{50}$$

where k is the Boltzmann constant.

Noise can also be computed by means of the Nyquist theorem[13]

$$\bar{e}_f^2 = 4kTR\frac{hf}{kT} \quad \frac{1}{e^{hf/kT} - 1} df \quad , \tag{51}$$

where e_f is the fluctuating e.m.f. in a small frequency interval df. For frequencies up to 10^{13} c.p.s. and at not

too low temperatures, $hf/kT \ll 1$, so that equation (51) becomes

$$\bar{e}_f^2 = 4\ k\ T\ R\ df \quad . \qquad (52)$$

The voltage on the capacitance, u_f, in the bandwidth df, if the inductance of the circuit is neglected, will be

$$u_f = \frac{e_f}{\left(R^2 + \frac{1}{\omega^2 C^2}\right)^{\frac{1}{2}}} \frac{1}{\omega C} \quad , \quad \omega = 2\pi f$$

and

$$u_f = \frac{e_f^2}{R^2\omega^2C^2 + 1} \quad , \qquad (53)$$

where R and C are the equivalent values of the resistance and the capacitance, respectively (fig. 5b).

To find the total mean square voltage $\bar{u}^2$ on the counter, equation (53) must be integrated over the whole frequency band, substituting previously for $\bar{e}_f^2$ its value from equation (52):

$$\bar{u}^2 = \int_0^\infty \frac{4\ k\ T\ R\ \ df}{R^2\omega^2C^2 + 1} \quad , \qquad (54)$$

which gives

$$\bar{u}^2 = \frac{k\ T}{C} \quad , \qquad (50)$$

which is identical to the value already obtained (eq. 50)

Since the response of a counter is an amount of charge, it would be useful to know the fluctuation of the charge which corresponds to the r.m.s. noise voltage. From equation (50) it follows

$$\bar{q}^2 = C^2\bar{u}^2 = C\,k\,T \quad , \tag{55}$$

to which, because of equation (2), corresponds a standard deviation in the energy spread

$$\overline{\Delta E}_\delta = \frac{\varepsilon}{e} \quad (CkT)^{\frac{1}{2}} \quad . \tag{56}$$

The energy resolution will be 2.35 times the standard deviation:

$$[\Delta E] = 2.35 \cdot [\Delta E]_\delta = 2.35 \cdot \frac{\varepsilon}{e} \quad (CkT)^{\frac{1}{2}} \tag{57}$$

It should be noted that [ΔE] (FWHM) depends only on the capacitance for a fixed temperature. For room temperature, if C is expressed in pF:

$$[\Delta E] \quad \text{FWHM} = 3.3 \sqrt{C} \quad \text{keV} \quad . \tag{58}$$

For our counter made of 400 ohm cm silicon with sensitive area of 5 mm^2 at a reverse bias of 100 volts, the pulse spread due to thermal noise is 7.4 keV (FWHM).

b. Current noise.

The current noise is due to the counter leakage current. There are three components of it: shot noise, generation-recombination noise and excess noise.

The shot noise is due to the fact that electric current is a flow of discrete charges of finite magnitude which are multiples of the electron charge e. If eω were infinitesimally small there would be no shot noise.

The shot noise is given by Schottky's formula[14]:

$$\bar{i}_f^2 = 2eIdf \quad , \tag{59}$$

where $\bar{i}_f^2$ is the current fluctuation (m.s.) and I the counter reverse current. The fluctuation of current gives a fluctuation of voltage on the load resistance whose m.s. value is

$$\bar{u}^2 = \int_0^\infty 2eI \quad \frac{R_L^2}{1 + \omega^2 C^2 R_L^2} \quad df \ . \tag{60}$$

Since

$$\int_0^\infty \frac{df}{1 + \omega^2 C^2 R_L^2} = \frac{1}{4R_L C} \ ,$$

it follows that

$$\bar{u}^2 = \frac{e \ I \ R_L}{2 \ C} \quad . \tag{61}$$

The corresponding noise charge has the following value:

$$\bar{q}^2 = C^2\bar{u}^2 = \frac{e\ I}{2}\ \tau \quad , \tag{62}$$

where τ is the circuit time constant: $\tau = R_L C$. Finally, for the standard deviation in energy we have

$$\Delta E_\delta^2 = \frac{\varepsilon^2}{e^2}\ \bar{q}^2 = \frac{\varepsilon^2}{2e}\ I\tau \tag{63}$$

and, if I is measured in μA and τ in microseconds:

$$E = 13.8\ \sqrt{I\tau}\ \text{keV}\quad (\text{FWHM}). \tag{64}$$

If the preamplifier time constant τa is shorter than $R_L C$ then τa should enter into the formulas (62) to (64). Then, from the above considerations it might be concluded that the shorter τa the better, so that τa could be as short as the carrier collection time in the counter. But F. S. Goulding and W. L. Hansen[15] showed that there is an optimum value for the amplifier time constant, because the r.m.s noise of the amplifier is inversely proportional to τa while that of the counter is directly proportional to it. This optimum time constant usually lies in the interval from 0.1 microseconds to 2 microseconds, depending on the system parameters.

The generation-recombination noise appears when the carriers in the counter can not cross from one electrode to the other without being trapped, or they recombine before

they are collected. Dearnaley and Northrop treated this kind of noise in their book[8] and showed that it may be neglected for junction counters when all the carriers cross the whole field region.

Very often in practice the current noise level of a counter is much higher than predicted by formula (64). This is because of the presence of so called excess noise. Relatively little is known about the nature of this kind of noise, and it is almost completely unpredictable. Its origin is the counter surface and the contacts. Thus, it depends on the surface treatment, but in a quite unpredictable way. Non-ohmic contacts also introduce excess noise.

It is known that the excess noise has 1/f frequency dependence, so that it is possible to reduce it by reducing the low frequency response of the amplifier.

In conclusion it may be said that, if the excess noise is absent, the total current noise of a counter is determined by equation (61) and its contribution to the energy resolution is given by equation (64).

1.6.3 Statistical fluctuations in ionization.

A particle of energy E will produce a certain number of electron-hole pairs in a counter, and this number is

$$N = \frac{E}{\varepsilon} \quad . \tag{65}$$

Let us consider a large number of monoenergetic particles incident on a counter. Because of statistical fluctuations, to every particle will correspond a different number of pairs. Assuming that the events which lead to the production of the pairs are mutually independent, which leads to a Poisson distribution of the numbers of pairs corresponding to the incident particles, the standard deviation of the spread of N wil be

$$\Delta N = \sqrt{N} \quad . \tag{66}$$

If all the pairs are collected the standard deviation of the collected charge is

$$\Delta Q = e \sqrt{N} \quad . \tag{67}$$

Because N is determined by equation (65) equation (67) may be written as

$$\Delta Q = e \sqrt{\frac{E}{\varepsilon}} \quad . \tag{68}$$

We are actually interested in the standard deviation of measured energies which corresponds to ΔQ. From equation (2) it follows that

$$\Delta Q = e.\frac{\Delta E}{\varepsilon}. \tag{69}$$

Combining equations (68) and (69) we get for the standard deviation in energy:

$$\Delta E_{\delta} = \sqrt{\varepsilon \cdot E} \quad . \tag{70}$$

To get energy resolution expressed as FWHM, when the distribution is Gaussian, equation (70) has to be multiplied by 2.35:

$$\Delta E = 2.35 \sqrt{\varepsilon \cdot E} \quad . \tag{71}$$

For 5.5 MeV particles the energy resolution due to the statistical fluctuations computed from equation (71) is:

$$[\Delta E] = 10.3 \text{ keV} \quad \text{(FWHM)}.$$

Fano showed[16] that, if the ionization events are not mutually independent, between the real spread and the spread given by equation (66) there exists the following relationship:

$$[\Delta N]^2_{\text{real}} = F\ [\Delta N]^2 \quad . \tag{72}$$

The number F (not to be confused with the electric field intensity F) is called the Fano factor. When there is no correlation between the ionizing events the factor F is equal to unity, otherwise it is always less than unity.

W. van Roosbroeck[1] explained that the ionizing events in semiconductors are correlated. He found a relationship between the Fano factor and the relative yield and number of phonons created per ionizing collision. Calculations based on his results and knowledge of the relative yield Y in the material ($Y = E_g/\varepsilon$, and it is about 30% for both Si and Ge), gives probable values for the Fano factor of 0.28 for silicon and 0.36 for germanium.

It should be mentioned that it was believed for a long time[8,17] that the Fano factor was not and should not be a different from unity.

S.O.W. Antman, D. A. Landis and R. H. Pehl[18,19] in 1965 measured the Fano factor for germanium using gamma rays and a Ge-lithium drift counter and obtained the value $F = 0.30 \pm 0.03$. The Fano factor for silicon was measured by O. Meyer and H. J. Langmann[20] using 1 MeV gamma rays incident on a 2 mm thick "basisfrei" silicon surface barrier counter. They obtained a value

$$F = 0.13 \pm 0.02,$$

considerably lower than the value predicted by van Roos-broeck's theory. This value will be accepted here and used later in the experimental part.

2. E X P E R I M E N T A L R E S U L T S

2.1 Manufacturing of the counters.

There are several manufacturing procedures of surface barrier counters but the basic principles are common for all. The aim of all manufacturing procedures is to form the barrier layer and make the contacts, one of which has to be an ohmic contact (on the base) and the other is the contact to the barrier layer.

Details of various manufacturing procedures may be found in references 21 to 25. Here will be given the main items of the method employed in this work.

In our work only counters with small sensitive areas were made, since they are most suitable for studying the energy resolution because of their low noise level.

a. Preparation of the wafers.

The starting material was 400 ohm cm n-type silicon in the form of slices 0.4 mm thick and about 2 cm in diamater, cut parallel to the (111) crystal plane. The slices had already been ground and lapped by the supplier. Many of the slices were broken during transportation into wafers of irregular shape.

Such a piece was taken, washed with detergent and put into concentrated nitric acid to soak for about ½ hour. Then it was rinsed in distilled water and dried on a piece of clean tissue paper.

b. Making of the base contact.

Such contacts were made on the base (back) surface of the wafer, opposite the face surface underneath which the barrier would be formed. It must be an ohmic contact. Special care has to be taken when making this contact because some important properties of the counter depend upon its quality.

It is very hard, or perhaps impossible, to make a contact to a semiconductor which would be perfectly ohmic. A real contact is always in between a rectifying and an ohmic contact, so that a practical ohmic contact is actually an approximation.

After step (a) was completed a piece of indium is applied to the back surface of the crystal by pressing and rubbing it with a small screwdriver until it adheres in a thin layer to the surface. A piece of insulated thin tinned copper wire was then soldered to the surface using indium as solder. Since the melting point of indium is 130°C, during the soldering process the crystal is not heated above 150°C, so that the carrier lifetime is not affected.

During the rest of the manufacturing procedure the soldered wire serves as a handle, which enables handling of the crystal without touching the crystal surface during the subsequent etching process and later. This is of particular importance, because it was found that touching the crystal surface is detrimental to the counter properties, e.g., the reverse current is increased and the breakdown voltage lowered as well as the energy resolution.

Contacts made in the above way are "non-injecting", as may be concluded from the shapes of the spectra presented. If there were appreciable carrier injection, the high energy side of the spectra would be distorted[18].

It should be mentioned that indium is a p-type impurity in silicon with an ionization energy of 0.16 eV. The fact that it makes good-non-injecting contacts on n-type silicon seems to be strange, and it was found empirically. Perhaps a mechanically damaged layer on the back surface plays the

main role here.

c. Etching.

Before etching, the back contact wire and the indium contact were covered with a thin layer of pure paraffin wax by means of a warm soldering iron.

Etching was done in CP-4A etch at $0^{\circ}C$ for about 6 minutes. Then, the crystal was washed with deionized water by successive dilution and decanting, and finally by a thin jet of deionized water.

The purpose of etching is to clean the crystal surface and take away the damaged surface layer.

d. Gold plating.

A very thin layer of gold was deposited on the crystal upper (front) surface by high vacuum evaporation through a mica mask. Care was taken that the mica mask, the purpose of which was to define the gold plated area, did not touch the crystal.

Several authors[21, 27] recommend a time interval of 6 hours to a few days between etching and gold plating, during which the crystal is exposed to air. It is supposed that an oxide layer is formed during this time, which supposedly plays a principal role in the formation of the barrier.

e. Mounting.

The crystal was mounted on a small plexiglass plate as was shown in fig. 6. The top contact to the gold layer was made of a very thin copper wire (gold wire would be more suitable) soldered to the gold layer by Wood's alloy as a solder. Special care was taken not to touch the gold layer with the soldering iron, which would have damaged it. During this process there was no danger of unsoldering the back contact because the melting point of Wood's alloy is only $70^{o}C$.

The above technique of making the top contact was chosen because there is some doubt that the usual way of making the contact by silver paste may result in the penetration of the silver paste through the gold layer and cause the counter to deteriorate.

The above technique resulted in stable counters, which, after they were stored for four months in an ordinary drawer, unprotected from dust, could stand reverse bias voltages up to 900 volts and had very good energy resolution.

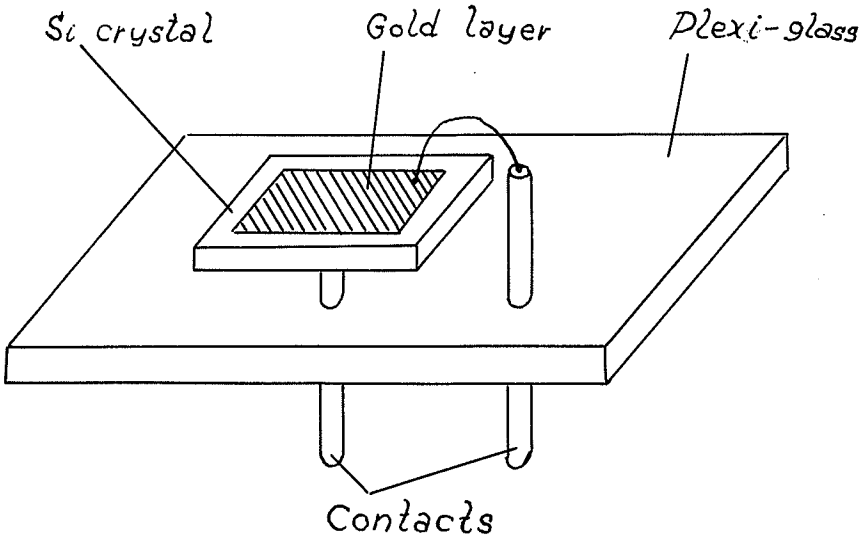

FIG. 6. SCHEMATIC DIAGRAM OF A FINISHED AND MOUNTED COUNTER;

2.2 Properties of the counters.

The sensitive areas of the counters were about 5 mm^2, and their thicknesses were around 300 microns. The resistivity of the material was 400 ± 40 ohm·cm (4 ohm·meter). The carrier lifetime was stated by the manufacturer to be roughly about 100 microseconds, but our measurements made by the photoconductivity decay method[28, 29] gave the value of about 15 microseconds. However, the samples on which the measurements were carried out were small and too thin, so that surface recombination may have played a major role in the measurements and caused the lifetime to appear lower.

Most of the counters could take high reverse bias voltages corresponding to the complete penetration of the depletion region to the back surface. Some of them could stand up to 900 volts reverse bias.

The best resolution at room temperature measured for 5.5 MeV alpha particles from A_M^{241} was 14.2 keV, and it is shown in Fig. 7. The reverse bias was 400 volts. The spectrum was taken without collimation. The resolution is equal to the best room temperature resolution for alpha particles, reported by Blankenship and Borkowski[27]. (It should be mentioned that 11 keV alpha particle resolution reported by G. G. George and E. M. Gunnersen[30] was not correctly evaluated, the real resolution being 14.1 kev).

High resolution of about 15 keV was maintained from 60 V bias up to 400 V bias (fig. 9). At 500 V the resolution was slightly poorer: 17 keV FWHM.

Since short term peak position shifts up to 5 keV were noticed, it is believed that a part of the resolution is due to drifts of the associated electronics.

The influence of collimation on resolution was examined. The resolution with collimation is shown in fig. 8, and it was 14.4 keV, about the same as without collimation. It is hard to conclude whether collimation improves resolution or not, because a much longer time is necessary to accumulate enough counts for the spectrum and, consequently, the chance for drift to spoil the resolution is higher.

The performances of the counters as high resolution alpha particle spectrometers are best illustrated by fig. 10, which shows an alpha particle spectrum of Am^{241} obtained in a 20 hour run. Five peaks are seen in the spectrum, including the one of 0.23% intensity. In order to make the low intensity peaks more prominent, the same spectrum is plotted on a logarithmic scale in fig. 11.

The spectrum was obtained without any collimation, the whole front surface of the counter being exposed to alpha particles. It is surprising that pulses due to the particles which strike the surface off the gold layer did not spoil the spectrum, swamping the low intensity peaks.

FIG. 7. BEST ENERGY RESOLUTION.

Counter: 4-19. Room temperature.
A_m^{241} alpha particles.
Bias: 400 volts

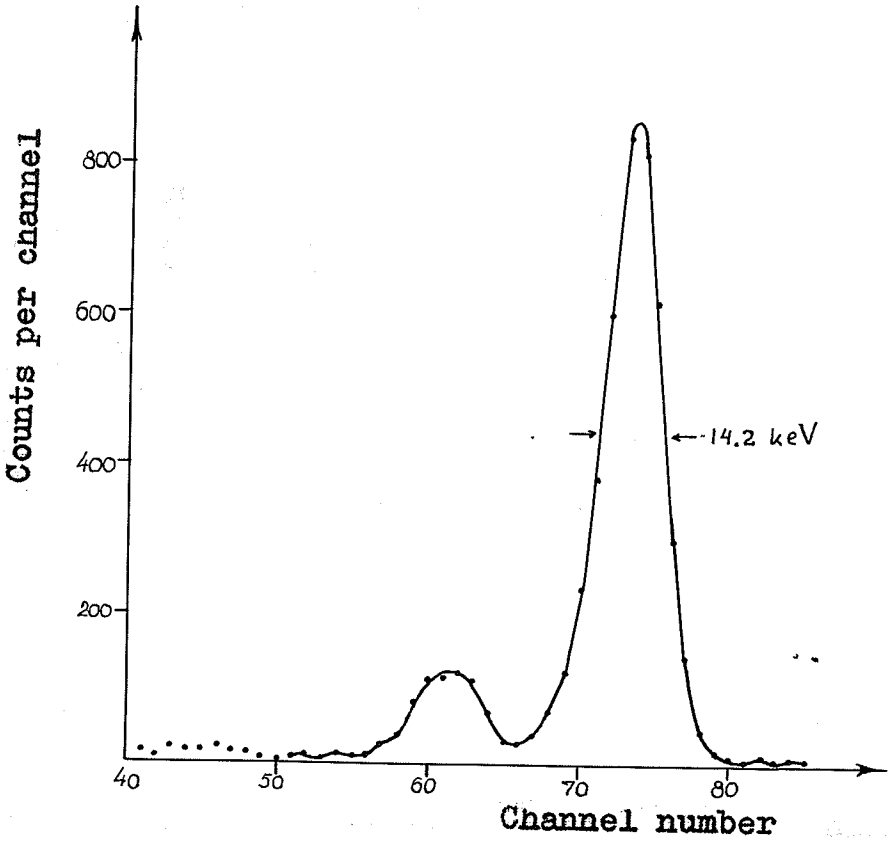

FIG. 8. INFLUENCE OF COLLIMATION ON RESOLUTION.

Counter: 4-19. Room tempr.
A_m^{241} alpha particles.
4 hour run.

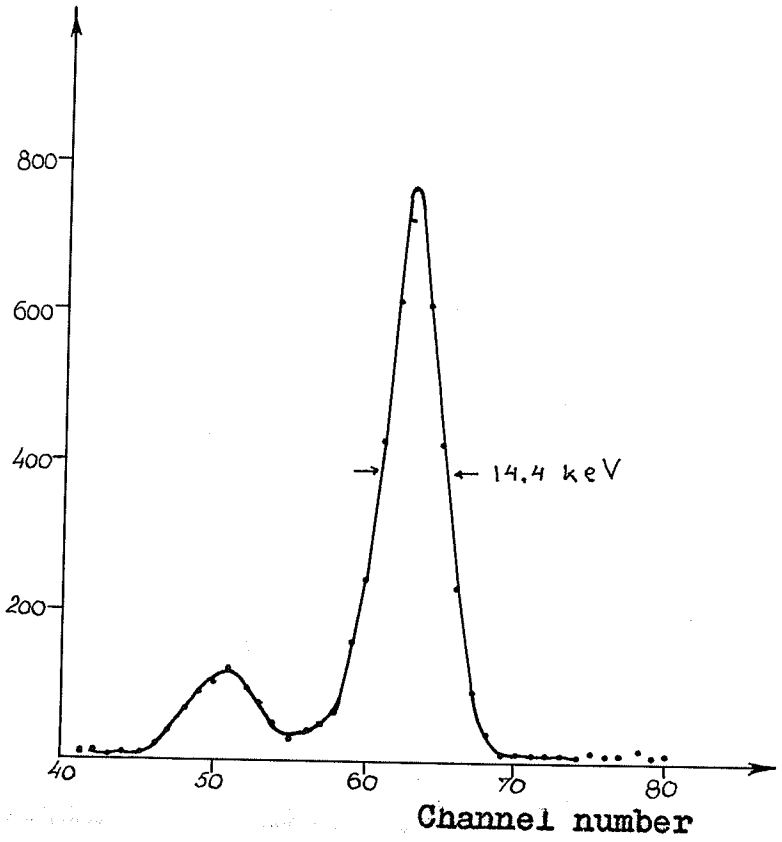

Fig. 9. DEPENDENCE OF ENERGY RESOLUTION ON BIAS VOLTAGE

Counter: 4-19
A_m^{241} alpha particles
Room temperature

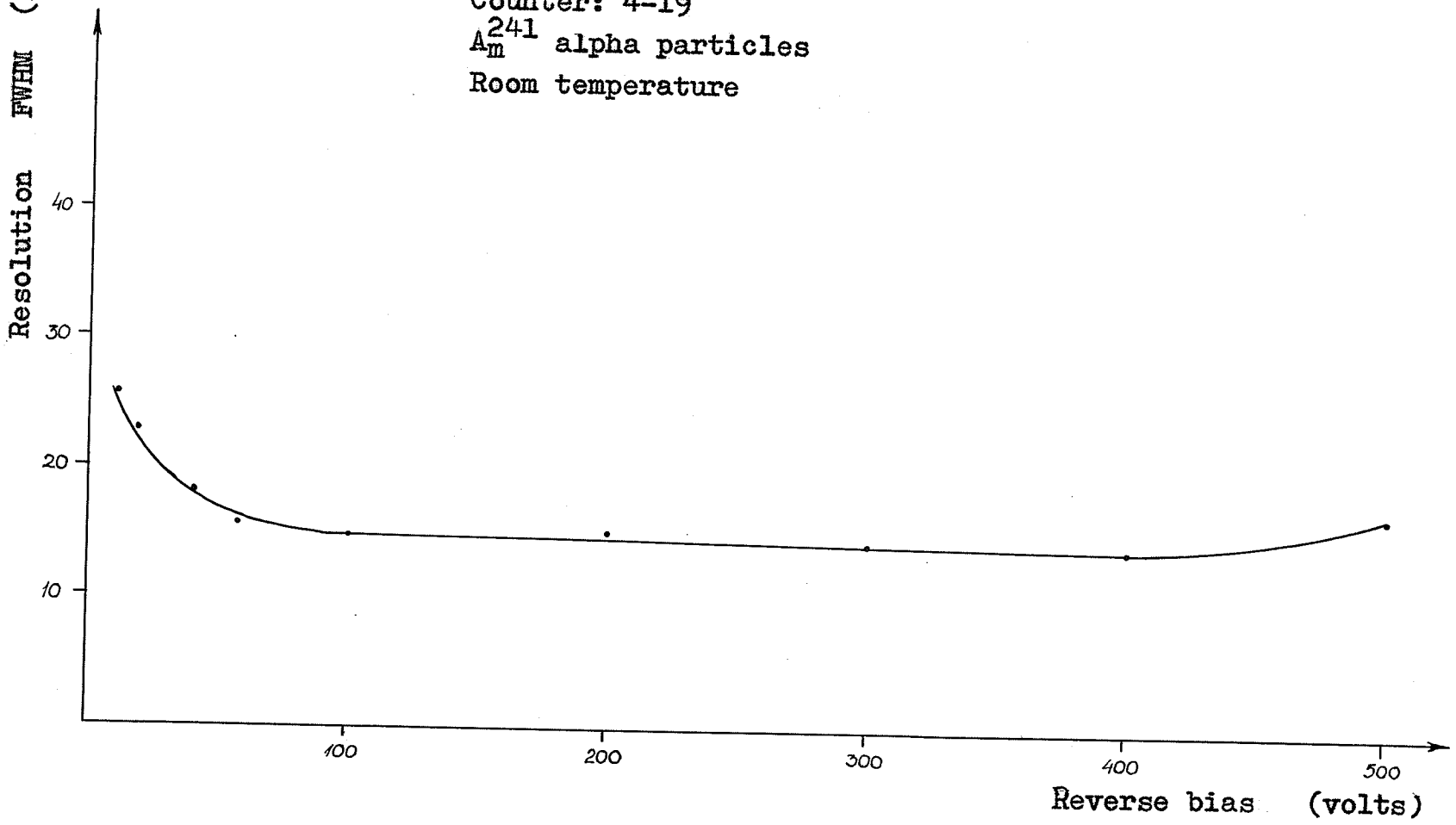

The energy separations among the peaks[31] agree well with the values obtained by the pulser, which is a confirmation that the counter together with the electronics had a linear response.

The results of examinations for some of the counters at various bias voltages are given in tables I to V.

It should be mentioned that the true bias voltage on a counter is obtained from the applied voltage by subtracting the voltage drop on the load resistor of 23 MΩ and adding the intrinsic voltage of 0.6 volts.

Examination of the counters was carried out by alpha particles from a thin A_m^{241} source. Energy spectra were taken using an ORTEC model 103 - 203 amplifier system and a CDC 100- channel pulse height analyzer.

FIG. 10. Am^{241} ALPHA PARTICLE SPECTRUM.

Counter: 4-19. Room temperature.
Bias: 400 volts.
20 hour run.

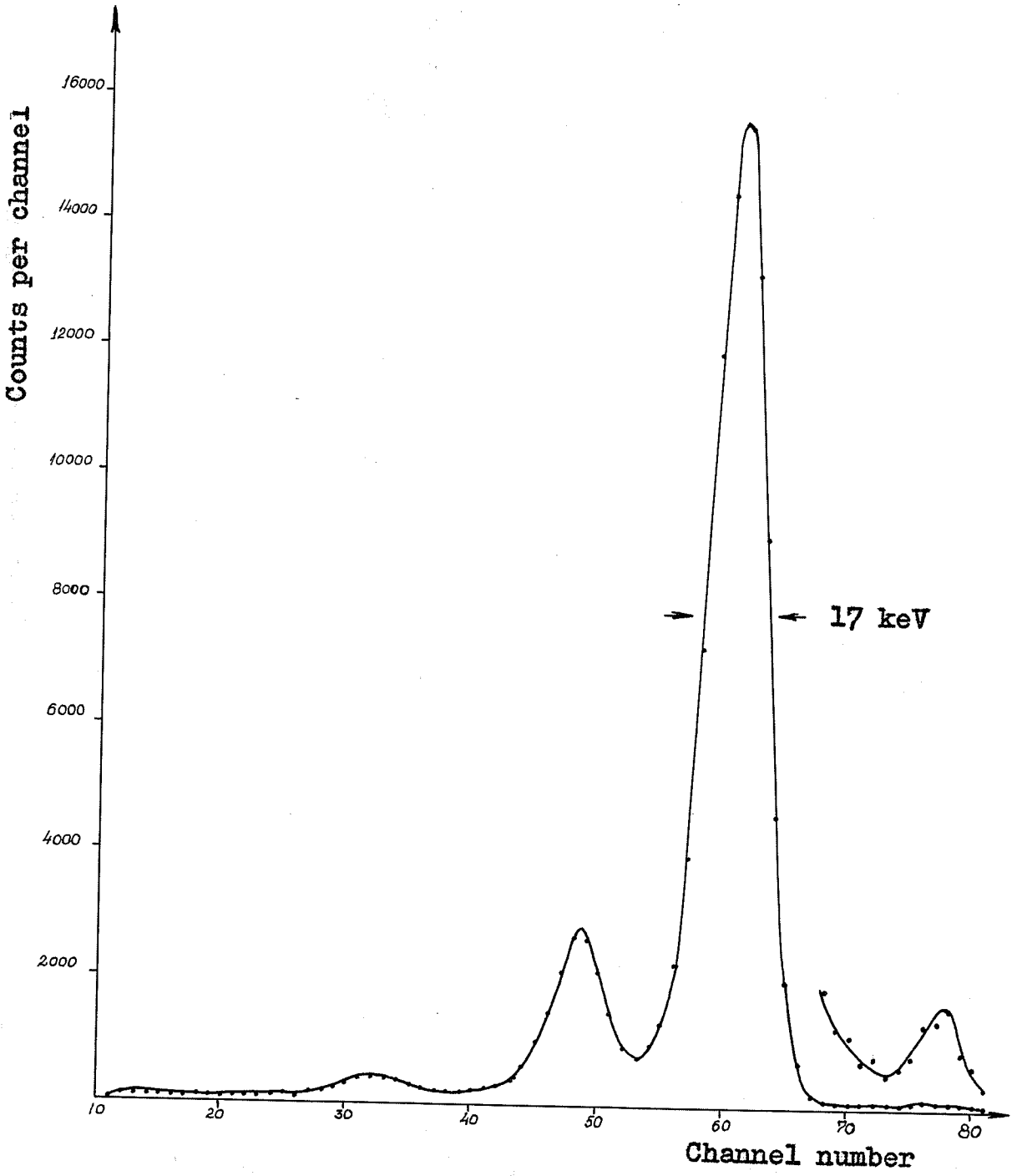

FIG. 11. A_m^{241} ALPHA PARTICLE SPECTRUM.
Counter: 4-19. Room temperature.
Bias: 400 volts.
20 hour run.

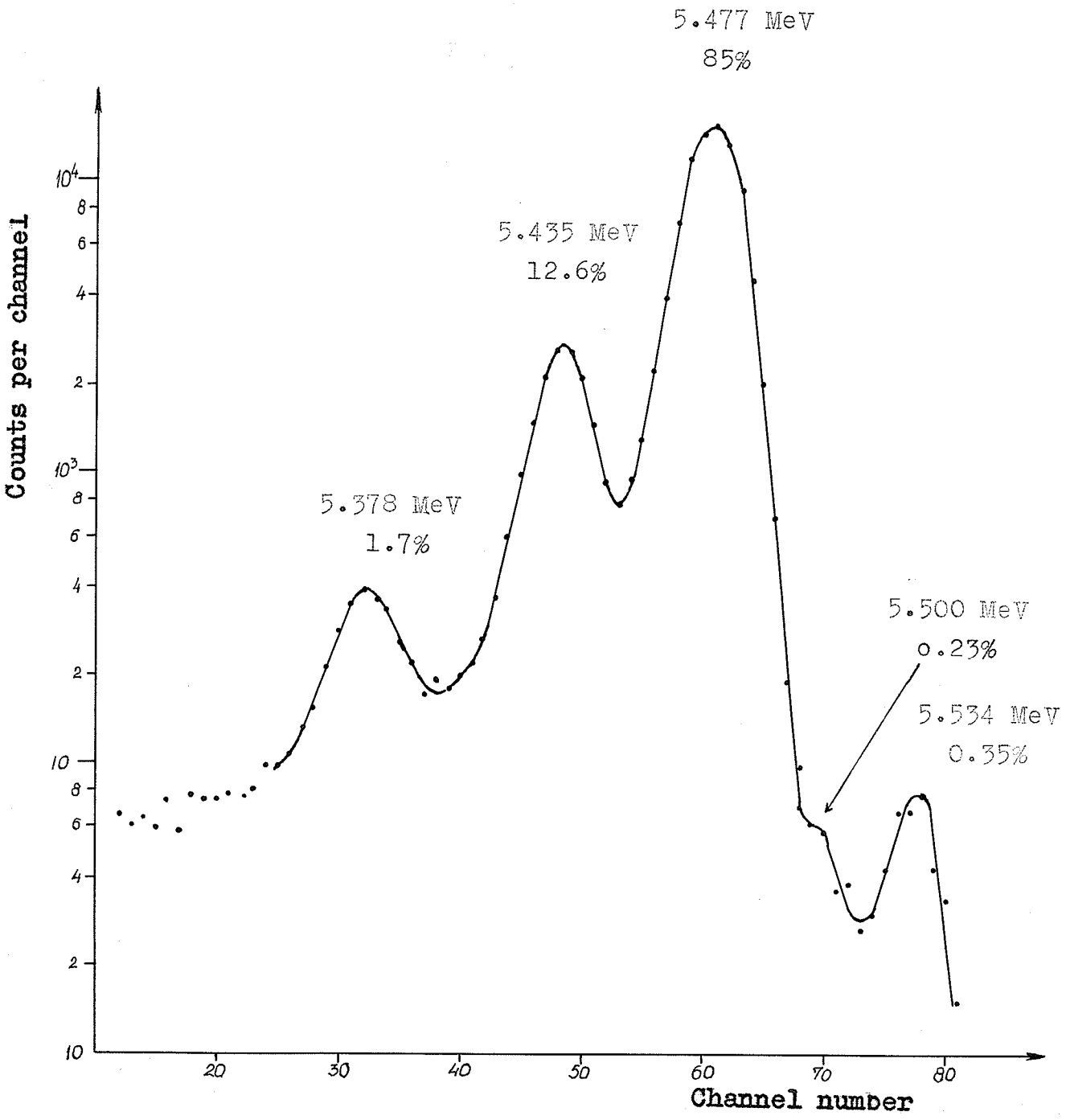

2.3 Reverse current and energy resolution.

There should be a correlation between the counter reverse current and the energy resolution, and, according to section 1.6.2b it should be determined by equation (64). However, in practice the relationship between these two quantities is more complicated, actually it is very often unpredictable, because of the presence of surface leakage current and the excess noise associated with it.

Only one counter had a reverse current in agreement with the value of the space charge generated current calculated from equation (32) on the basis of 15 micro-seconds carrier lifetime,and that was the counter with the best energy resolution.

Experience with our counters shows that two counters with approximately the same currents may have very different energy resolutions. This irreproducibility makes the studying of semiconductor counters very difficult.

In order to get rid of the surface leakage current, which is believed to be the cause of the irreproducibility, some authors[32] began constructing guard ring counters, where the surface leakage current is almost eliminated.

The best performances of guard ring counters are not better than the best performances of ordinary counters. Thus, it is open to question what is easier to do in order to get a good counter, whether to make one elaborate guard

ring counter or to produce four or five simple counters instead, and select the best one among them, which can be as good as the guard ring one. Therefore, it is not pointless to investigate ordinary counters with regard to reverse current.

Investigation of the noise contribution to the energy resolution was carried out by means of the ORTEC mercury relay pulser which was incorporated in the system. The FWHM of the pulser spectrum taken with the counter properly biased and placed at the input of the preamplifier gives the sum of all componets of the noise in the energy resolution:

$$[\Delta E]^2_{noise} = [\Delta E]^2_{current} + [\Delta E]^2_{thermal} + [\Delta E]^2_{electronics}$$

where the symbols are self-explanatory. When there is no excess noise, the first term on the right side, the current noise, may be computed from equation (64) and the second term, the thermal noise, may be calculated from equation (58). The value of the electronics noise is obtained by means of the pulser spectrum when a condenser is placed at the input of the preamplifier[33].

At low biases the noise is high because of the large value of the detector capacitance. When the bias increases

this noise decreases but the component of noise due to the reverse current starts to increase. Therefore, there should be a minimum of noise at a certain bias.

The calculated and observed values of noise are presented in columns 5-6 of tables I to V. The calculated values of noise were obtained assuming that there was no excess noise (which could not be calculated). There is a good agreement between observed and calculated values for counter 4-19 except at biases above 400 volts. There is also a fair agreement for counter 4-8 at low biases, while at biases above 50 volts the discrepancy is larger. But for other counters the discrepancies between observed and calculated values are large, indicating that the excess noise is high.

It should be noted that in both cases where there was agreement between calculated and observed values of noise, the counters had very good energy resolutions, about 15 keV and about 25 keV respectively. However, one of the counters had a reverse current in accordance with the theory, while the current of the other was an order of magnitude higher.

A very interesting fact was noticed concerning the reverse current and the energy resolution. It consists of the following.

It was observed that a counter one day may have one

energy resolution and another day a different value. These changes of resolution were always accompanied by changes of the reverse current. The changes seemed to be quite unpredictable and for a long time it was not known what was causing them, until it was found out that if a counter had poorer resolution one day and it was left over night in the chamber, the next morning it had better resolution and lower reverse current! Soon it was found that the effect was the same whether the counter was left in the chamber with the reverse bias on and in vacuum, or without bias and at atmospheric pressure. Of course, because of the photosensitivity all the experiments were performed in darkness.

The following fact was established definitely: when the counter was previously exposed to light and then closed in the chamber, its resolution deteriorated and the reverse current was higher. The breakdown voltage was lowered, too. In darkness the resolution improves with time and the reverse current decreases. A stationary state with the best resolution and the lowest reverse current is reached after a period of 12 to 24 hours, and sometimes even longer. For brevity we shall refer further to this effect as the "the photo irradiation effect" (p. i effect). The state of a counter in which the effect is present will be designated as the "p. i. state" as a contrast to

the "normal state" in which the reverse current is lowest and the resolution has its best value.

The current-voltage characteristics of counter 4-19 in the normal and the p. i. states are presented in fig. 12 (page 69).

The following table, in which the data for counter 4-19 are given, may serve as an illustration of the difference between the normal state and the photo irradiation state:

Applied voltage	i_{rev} uA	Bias voltage	Resolution keV	Noise		$[\Delta E]_D$ keV
				measured keV	calculated keV	
N o r m a l S t a t e						
100	0.067	99	15.1	10	9.8	11.8
200	0.085	198	15.4	9.6	9.0	11.4
p. i s t a t e						
100	0.35	92	32.2	14.5	13.0	28.6
200	0.55	188	27.6	15.5	13.9	22.6

The meaning of $[\Delta E]_D$ will be explained later.

It is to be noted from the above data that the

measured values of noise agree well with calculated values both in the normal state and in the P. i. state, that is, to the higher value of i_{rev} in the p. i. state corresponds appropriately higher value of noise. However, the energy resolution is poorer in the p. i. state than follows from the noise increase. We shall return to this point later.

FIG. 12. CURRENT - VOLTAGE CHARACTERISTICS IN THE NORMAL AND THE p.i. STATES.

COUNTER: 4-19. Room temperature.

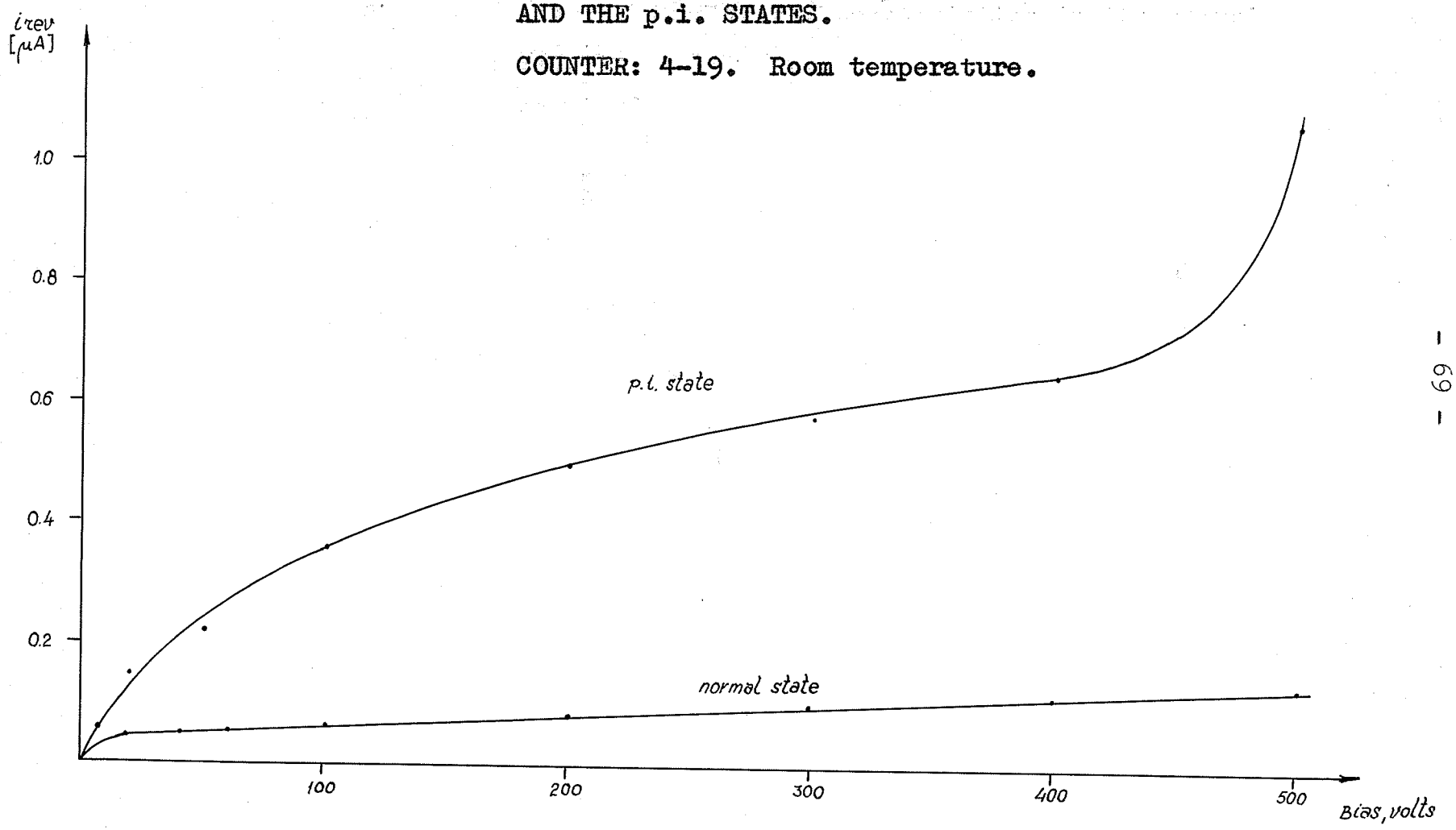

There seems to be no easy explanation for the p. i. effect. One possibility may be that the slow surface states are excited. This is suggested by the value of the relaxation time of these states, which is of the same order of magnitude as the time required by a counter to come from the p. i. state into the normal state.

Several authors mention instabilities of surface barrier counters. It is quite possible that the p. i. effect is responsible for some, if not for all instabilities. Our counters were very stable in the normal state, having fully defined resolution and reverse current at a given voltage. The only instability was caused by irradiation with light, which was manifested in the above manner.

2.4 Charge collection efficiency and resolution.

Comparing the ultimate resolutions obtained with densely ionizing particles such as alpha particles or heavy ions, 14 to 15 keV, with the ultimate resolutions obtained with energetic electrons or gamma rays, 4 to 5 keV, one can observe the fact that the peak widths of heavy particles are much wider. It is reasonable to ask: why is this so? The next question should be: could not it be, perhaps,

connected with the ionization density along the initial particle track? The fact that the energy resolution for alpha particles is not limited by noise was revealed at the Ashville conference[32] and explicitly stated in the discussion by J. M. McKenzie.

As was mentioned earlier the maximum energy of electrons knocked by a heavy particle, which are called delta rays, is quite small, of the order of a few eV, so that their range is very short. A consequence of this is that all the electron-hole pairs are created in a narrow cylindrical region around the particle track. The diameter of this cylinder is of the order of one micron for alpha particles[34], and the density of electron-hole pairs in it about 10^{16} pairs/cm^3, so that they form a sort of plasma region around the particle track.[35]

The implications of this high density plasma are twofold. First, the value of carrier lifetime in the plasma region is unknown since the concept of carrier lifetime is derived for the case when the excess carrier concentration is small compared to the existing concentration; but it is likely to be greatly diminished. Second, the electric field in the counter, which is supposed to separate the carriers of opposite signs and sweep them across, is distorted around the high conductivity plasma region, in which it is reduced to zero. Carrier collection is accomplished

by erosion of the plasma periphery, enhanced by diffusion. This extends the collection time, as was observed experimentally in the case of fission fragments[36]. Both of the consequences act in the same direction: they impair the charge collection, since the collection is prolonged and the lifetime decreased simultaneously.

Because of the above reasons, there should be a pulse height defect in the spectra of densely ionizing particles, which was really observed for fission fragments by several authors[37, 38, 39]. A great deal of discussion at the Ashville conference on semiconductor detectors was devoted to this matter which seemed to have embarassed the workers in the field, since it was believed that the charge collection efficiency in semiconductor detectors was 100%.

For alpha particles the pulse height defect was observed only after irradiation by large doses of neutrons or electrons[30]. Degradation of the energy resolution was observed at the same time.

Our results show that collection efficiency, μ , for alpha particles is not exactly 100% even at high bias voltages such as 400 volts or higher. This is shown in fig. 13, where μ is arbitrarily taken to be 100% at 500 volts bias. The points of the curve were plotted after the effect of pulse height shift due to the capacitance changes with bias was subtracted. Similar pulse height defect was reported

by E. Baldinger and W. Czaja[40].

It seems that this pulse height defect is due to carrier recombination in the high density plasma region of the initial particle track, because it decreases with increasing the electric field intensity in the counter. The percent pulse height defect, which is equal to 100 - μ%, is plotted in fig. 14, against the electric field intensity, F_R, at the end of the 5.5 MeV alpha particle track. The values of F_R are obtained from formulas (23) and (24) (see also fig. 3 and fig. 4).

It is not likely that the pulse height increases with bias (fig. 13) because of a multiplication process, such as would occur due to carrier injection by the back contact, since the energy spectra are not distorted and the energy resolution is good even at 500 volts bias.

An attempt was made to correlate the collection efficiency (or the pulse height defect) with the energy resolution. To this effect, the resolution was measured for several counters as a function of the reverse bias voltage. The results are presented in column 4 of tables I to V and also in fig. 9.

The energy resolution may be calculated by means of the formulas given in section 1.6 if the contributions by the noise and by the statistical fluctuations are known. The noise contribution can be measured by a pulser (see section 2.3),

FIG. 13. CHARGE COLLECTION EFFICIENCY AS A FUNCTION OF THE REVERSE BIAS VOLTAGE.

Counter: 4-19. Room temperature.
A_m^{241} alpha particles.

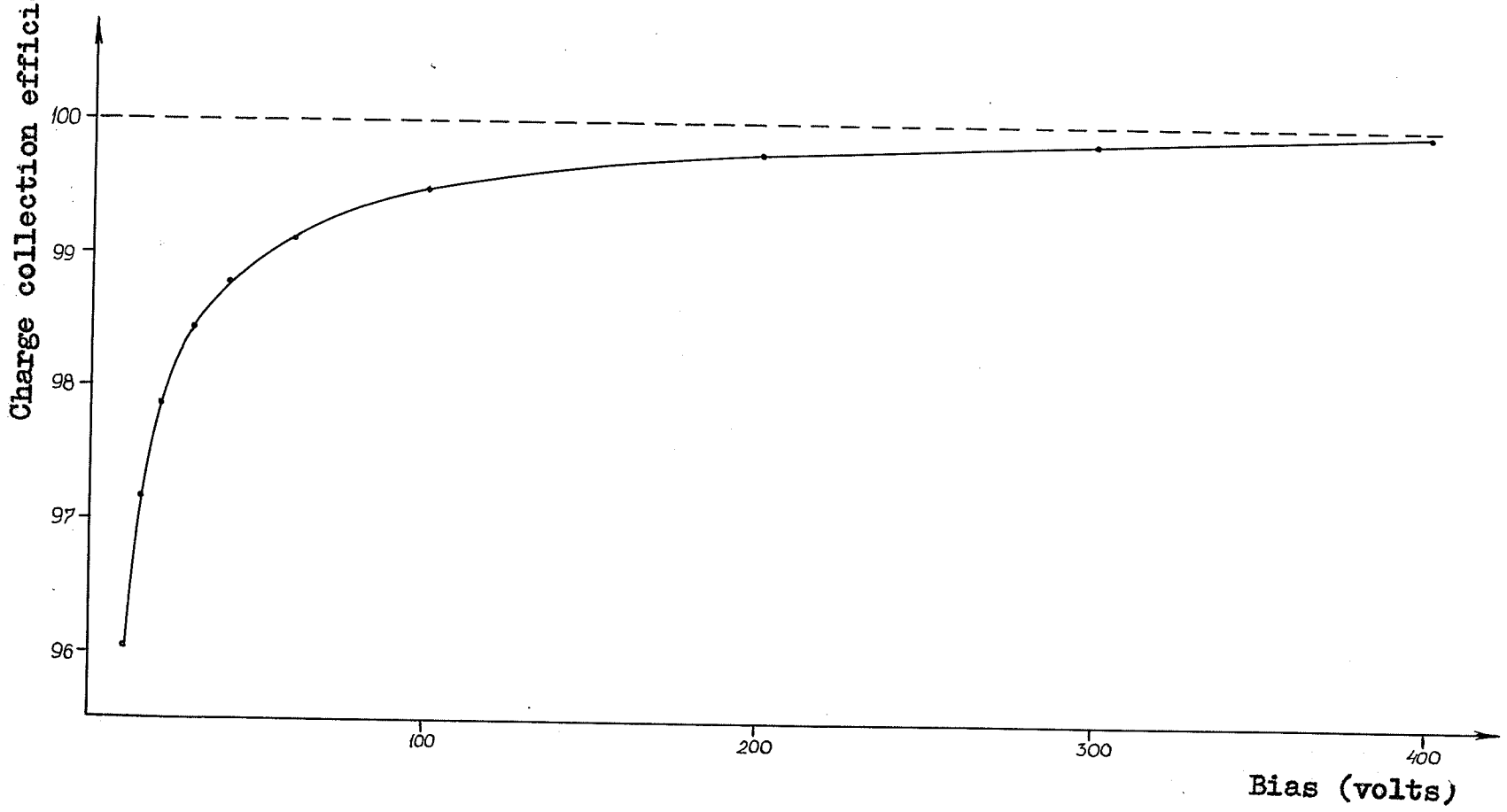

FIG. 14. Pulse height defect for 5.5 MeV alpha particles as a function of the electric field intensity F_R at the end of the track.

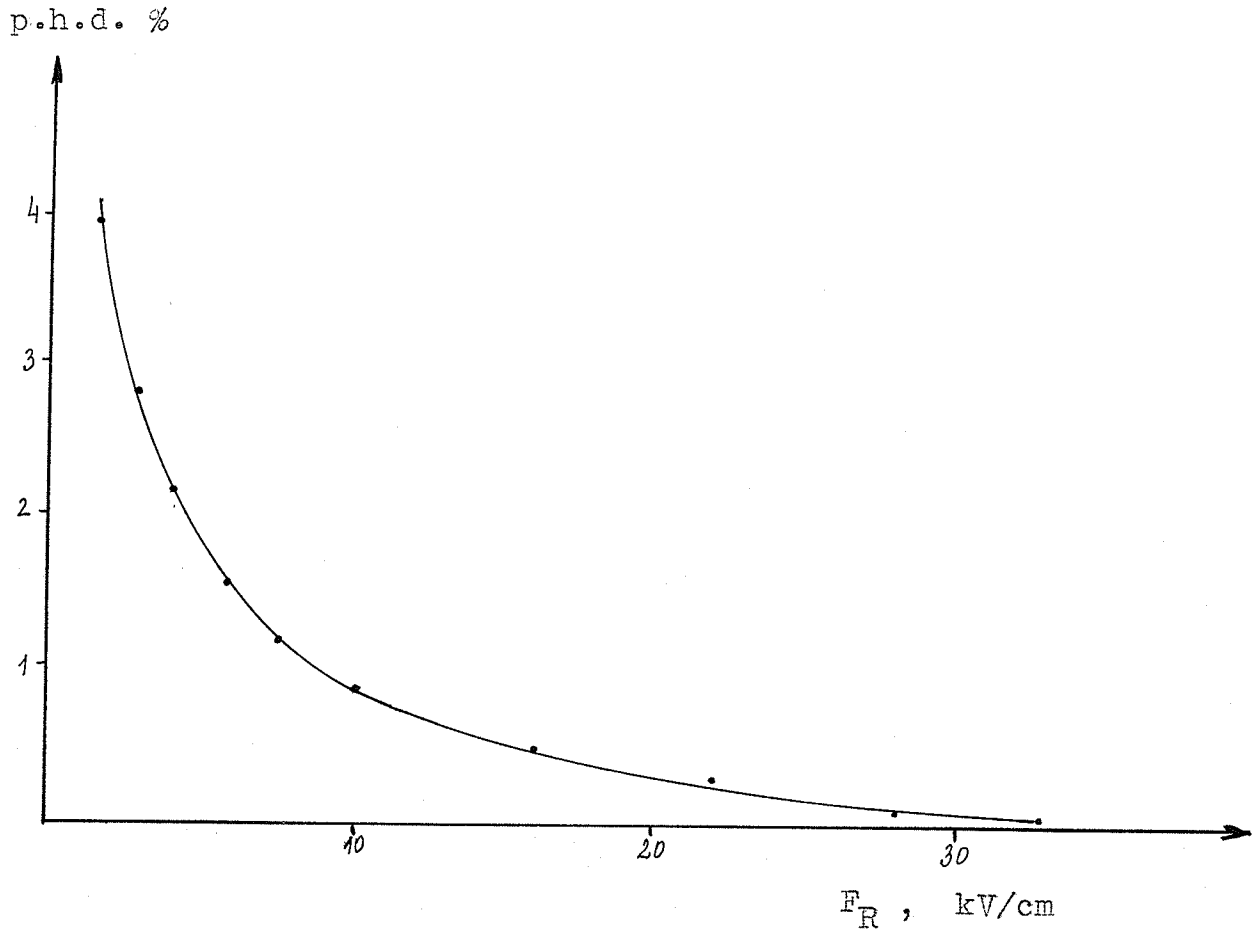

while the statistical component can be computed from equation (71) making use of equation (72) and using the value of the Fano factor $F = 0.13$:

$$[\Delta E]_S = 3.75 \text{ keV} \quad \text{FWHM}.$$

If we designate by $[\Delta E]_{calculated}$ the calculated value of resolution and by $[\Delta E]_n$ the noise contribution then

$$[\Delta E]^2_{calculated} = [\Delta E]^2_n + [\Delta E]^2_s$$

In the case of alpha particles there is always a discrepancy between measured and calculated values of resolution, measured values being always larger than the calculated ones, which means that there is an additional unknown contribution to the resolution. We shall call the unknown component of resolution "the resolution discrepancy", $[\ E]_D$. We have:

$$[\Delta E]^2_D = [\Delta E]^2_{measured} - [\Delta E]^2_{calculated}$$

The resolution discrepancy for various counters and biases is given in column 7 of tables I to V and it is represented graphically as a function of bias for two of the counters in fig. 15 and fig. 16. It is seen that the best resolution counter 4-19 had the lowest value of the discrepancy.

It is reasonable to suppose that, if there were any effect of charge collection efficiency on energy resolution, it should be easiest to discover it in the best resolution counter, where the possibility for it to be masked by other effects is lowest.

Fig. 17 shows the plot of logarithm of the resolution discrepancy versus charge collection afficiency for counter 4-19. It appears to be a straight line. The points on the graph, from left to right, correspond to the following bias voltages, respectively: 5, 10, 20, 40, 60, 100, 200, 300 and 400 volts. The last (lowest) two points which are off the straight line belong to the highest voltages.

A conclusion that could be made is that the resolution discrepancy $[\Delta E]_D$ or one component of it is due to carrier recombination or trapping. It is seen in fig. 15 that $[\Delta E]_D$ decreases with increasing bias voltage up to about 100 volts. From 100 volts to 400 volts it is constant. Above 400 volts (not shown in the graph) $[\Delta E]_D$ begins to increase, having the value 11.2 keV at 400 volts and

FIG. 15. RESOLUTION DISCREPANCY, $[\Delta E]_D$, AS A FUNCTION OF THE BIAS VOLTAGE.

Counter: 4-19. Room temperature.
A_m^{241} alpha particles.

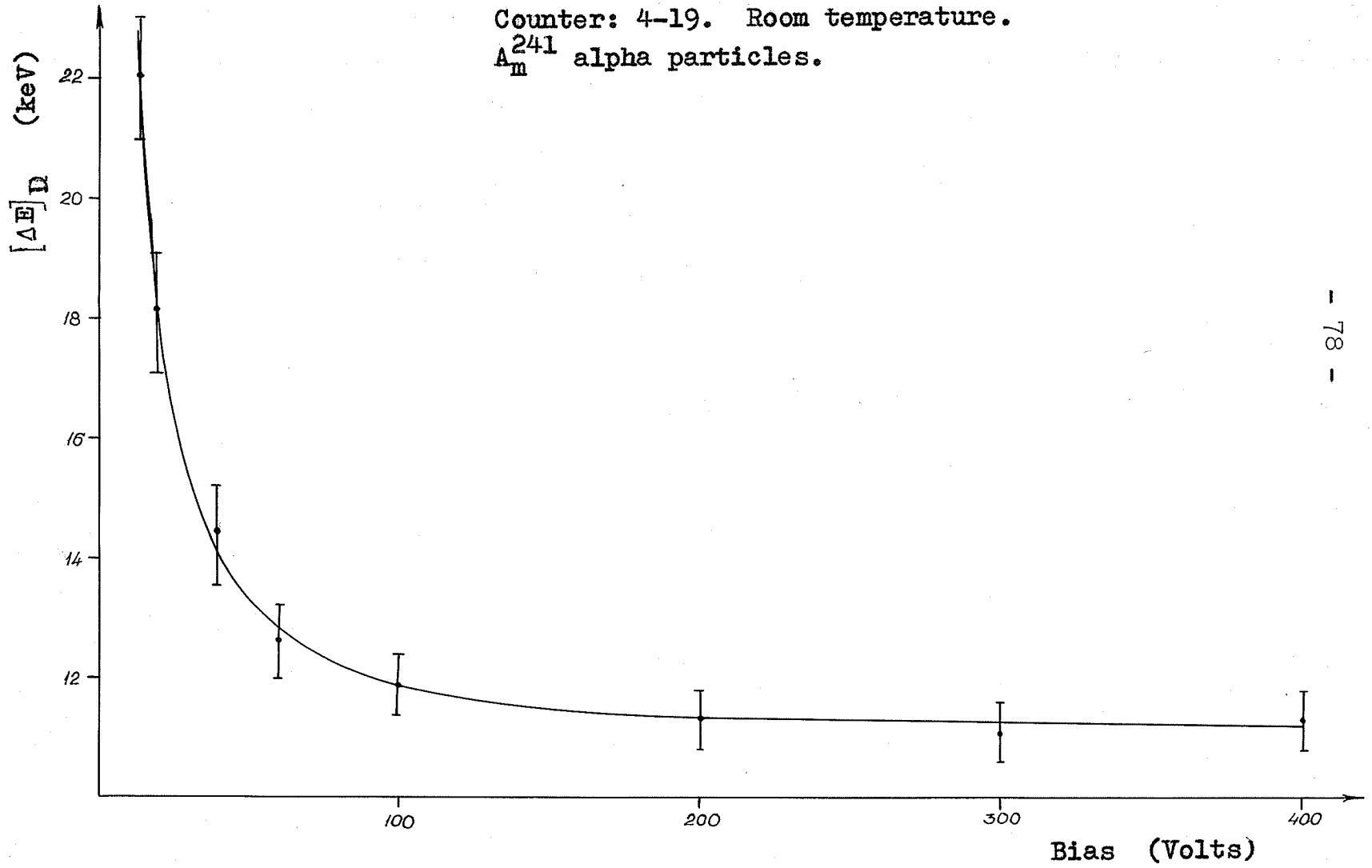

FIG. 16. RESOLUTION DISCREPENCY $[\Delta E]_D$ AS A FUNCTION OF THE REVERSE BIAS VOLTAGE.

Counter: 4-18. Room temperature.
A_m^{241} alpha particles.

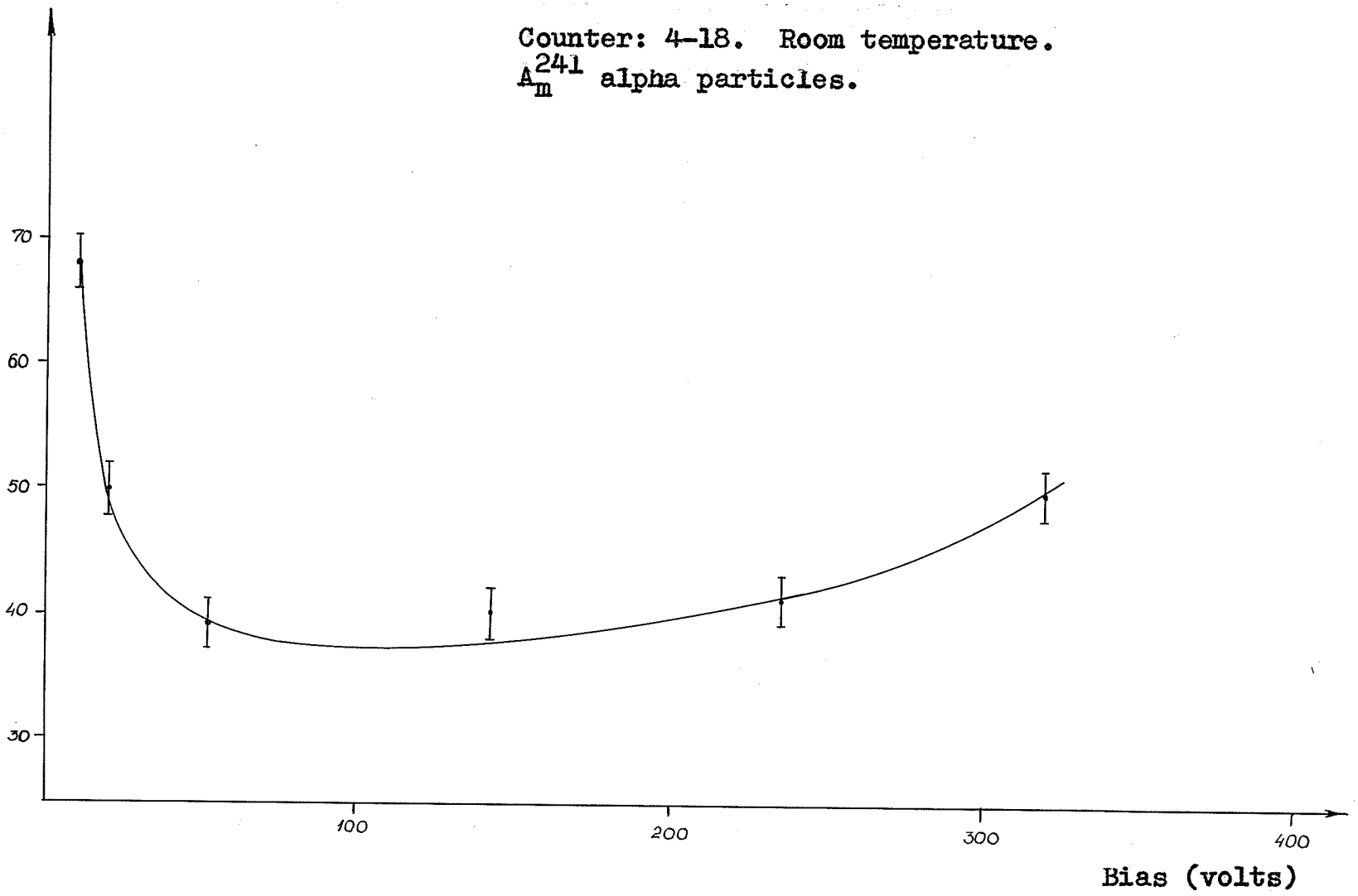

FIG. 17. RESOLUTION DISCREPANCY AS A FUNCTION OF CHARGE COLLECTION EFFICIENCY.

Counter: 4-19. Room tempr.
A_m^{241} alpha particles.

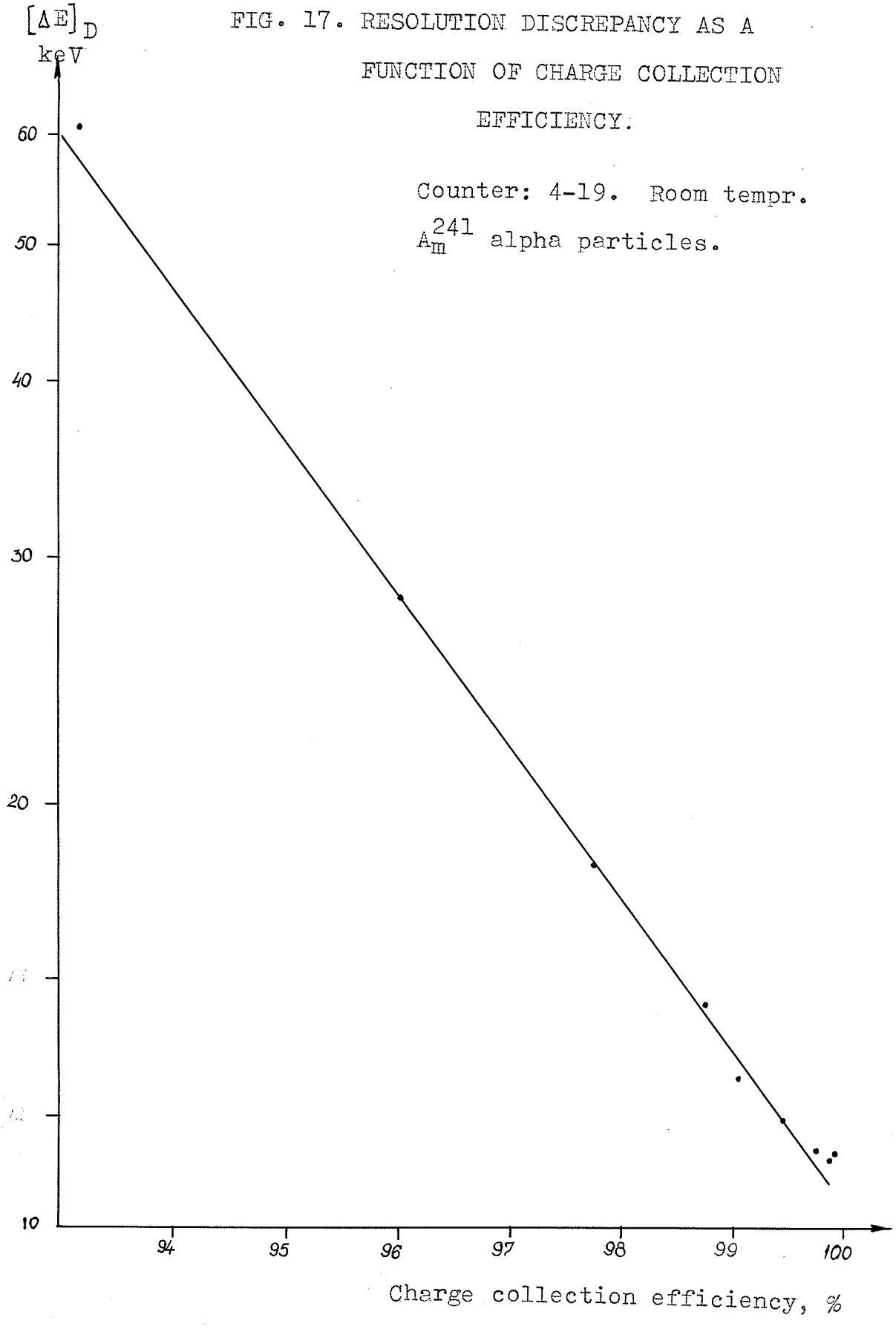

13.4 keV at 500 volts (table I). In counters with poorer resolutions $[\Delta E]_D$ begins to increase even at much lower biases (fig. 16).

How can the increase of $[\Delta E]_D$ with bias voltage be explained? Obviously there is a component of it, $[\Delta E]_D^{\cdot}$, which increases with bias. $[\Delta E]_D^{\cdot}$ could come from some sort of charge multiplication, the effect of which is larger at higher bias voltages.

It is hard to say what is the origin of the charge multiplication: whether it comes from some small local surface breakdowns of very short duration, caused by impinging particles, or it comes from contact injection. Perhaps, some clue may be provided by closer investigation of the p. i. state, since the p. i. state is connected with $[\Delta E]_D$. Namely, $[\Delta E]_D$ is much larger in the p. i. state than in the normal state (see last column in the table on page 68).

The change of the energy resolution with bias voltage, at low biases, is illustrated in fig. 18.

2.5 Counters made of heated silicon.

It was discovered[41] that when silicon is heated to temperatures above 500°C and then quenched, its carrier lifetime is much lower than before the heating.

We used the above method to obtain some silicon wafers with low carrier lifetime, which were then used for making counters. The wafers were heated to 550°C for 5 min. and then quenched in vacuum oil. The photoconductivity method of carrier lifetime measurement gave values of about 2 microseconds for the carrier lifetime in the wafers. Surface barrier counters were made of the wafers by the method described in sec. 21.

The counters made of heated and quenched material had about the same performances as the counters made of the original material. Only three counters were made this way. One of them had an energy resolution with alpha particles as good as 22 keV.

The main purpose of making these counters was to see whether their resolution discrepancy was larger than in the case of normal counters. Somewhat surprisingly, it was found that $[\Delta E]_D$ was approximately the same as in normal counters.

Detailed examination of the counters made of heated

FIG. 18. CHANGE OF THE ENERGY RESOLUTION WITH THE REVERSE BIAS VOLTAGE.

Counter: 4-19. Room temperature.
A_m^{241} alpha particles.

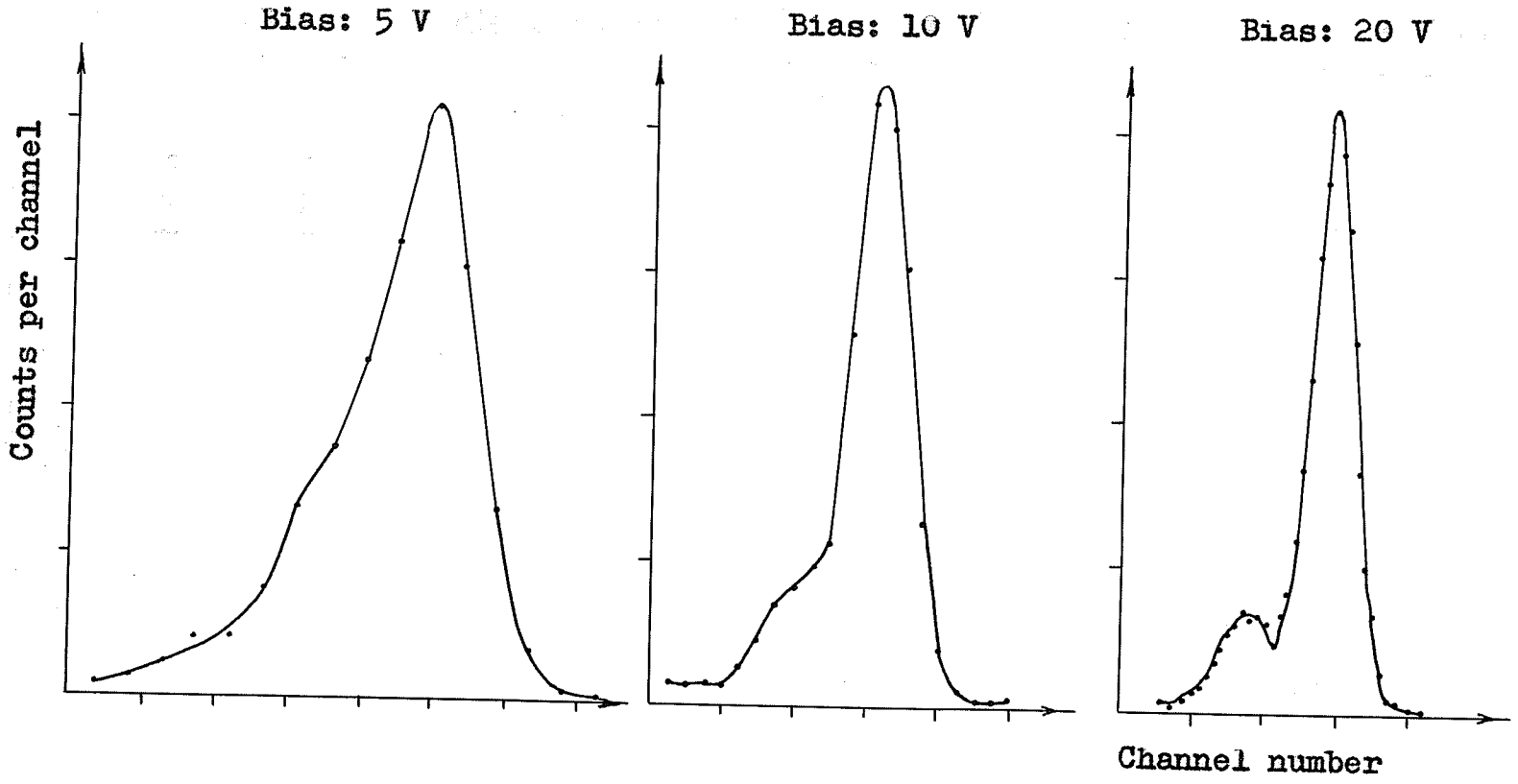

and quenched silicon could not have been carried out because all three were damaged mechanically by accident.

2.6 Summary of results and conclusions.

A number of counters was made with both of the contacts soldered. The counters had good performances.

The best resolution attained with 5.5 MeV alpha particles was 14.2 keV FWHM and in a 20 hour run 17 keV FWHM.

After irradiation with light, the counter reverse current (in darkness) increased (up to 10 times in some cases) and the energy resolution deteriorated. The reverse current and the resolution returned to the original values after one to two days. The effect was reproducible.

The charge collection efficiency was not 100%, but depended on the electric field intensity in the counter. The effect is equally pronounced in high resolution counters and low resolution counters.

There is a discrepancy between the observed values of energy resolution and the values calculated from the noise level and the statistical fluctuations of ionization (taking the Fano factor to be 0.13). The discrepancy consists of two

components. One component is dominant at lower collecting field intensities, and it is believed to be due to carrier recombination in the plasma region along the initial particle track. There is a linear relationship between the logarithm of this component and the collection efficiency (fig. 17) or the pulse height defect. The other component of the resolution discrepancy increases with the reverse bias, and it might be due to some sort of carrier multiplication.

The counters made of heated and quenched silicon had the same properties as the normal counters.

Table I.

Counter: 4-19. A_m^{241} alpha particles. Room temperature.

Applied voltage	i_{rev} uA	Bias volts	Resolution keV	Noise		Resolution discrepancy keV
				measur. keV	calcul. keV	
1.	2.	3.	4.	5.	6.	7.
5	0.026	4.4	55	19	14	46
10	0.032	9.3	32.5	16	13.6	28
20	0.036	19.2	22.8	13.4	11.9	18.1
40	0.043	39	21.5	12.1	11.2	17.4
60	0.058	59	16	10.1	10.3	12.6
100	0.067	99	15.2	9.6	9.8	11.8
200	0.085	199	15.4	9.8	9.0	11.3
300	0.092	298	15.4	9.7	8.8	11.2
400	0.11	398	15.3	9.6	8.6	11.2
500	0.12	498	17	13.4	8.6	13.4

Tables II and III.

Am^{241} alpha particles. Room temperature.

Applied voltage	i_{rev} uA	Bias volts	Resolution keV	Noise		Resolution discrepancy keV
				measur. keV	calcul. keV	
1.	2.	3.	4.	5.	6.	7.
Counter 4-8						
15	0.34	7.3	45	19.5	16.7	40.4
20	0.42	10.3	27.6	19	16.6	19.7
30	0.52	18.2	26	18	15.9	18.4
50	0.69	34	26.8	18	16	19.5
70	0.85	50	25.4	-	-	-
100	1.05	76	27.0	18.4	17.1	19.3
150	1.55	115	37	29	19.4	23
Counter 4-L2						
35	1.3	5	153	52	23	144
40	1.35	9	88	50	21.3	73
60	1.8	19	73.5	50.5	22.2	53
100	2.2	50	71	56.8	22.8	42.8
200	2.9	133	74	59.6	24.8	43.6

Tables IV and V.

A_m^{241} alpha particles. Room temperature.

Applied voltage	i_{rev} uA	Bias volts	Resolution keV	Noise		Resolution discrepancy keV
				measur. keV	calcul. keV	
1.	2	3.	4.	5.	6.	7.
Counter 4-18						
40	1.4	5	151	62,5	23.3	137
60	1.6	20	72	51.8	21.4	50
100	2.1	52	71	59	22.2	39
200	2.6	143	76.5	65.5	23.6	40.4
300	2.8	235	74	61	25	41.5
400	3.5	320	80	62,5	27.3	50
Counter 4-14						
30	0.92	9	58.2	28	20.0	50.8
50	1.33	19.5	38.2	28.8	20.7	24.8
100	2.1	51	61.5	50.5	23.0	35.0
190	3.15	118	98	89.5	26.4	40.0

R E F E R E N C E S

1. W. van Roosbroeck, Phys. Rev. 139, A1702; 1965.
2. K. G. McKay and K. B. McAfee, Phys. Rev. 91, 1079; 1953.
3. H. O. Funsten, Trans. IRE vol. NS-9, 190; 1962.
4. W. D. Davis, J. Appl. Phys. 29, 231; 1958.
5. I. E. Tamm, Physik Z. Sowjetunion 1, 733; 1932.
6. R. J. Fox and C. J. Borkowski, Trans IRE vol. NS-9, 213-216; 1962.
7. E. D. Klema, Nuclear Instr. and Methods 26, 205-208; 1964.
8. G. Dearnaley, D. C. Northrop, Semiconductor Counters For Nuclear Radiations,(Spon, London, 1963).
9. W. L. Brown, Proc. Asheville Conference, NAS-NRC Publication, vol. 871, 9-14; 1961.
10. H. K. Henish, Rectifying Semi-Conductor Contacts, (The Clarendon Press, Oxford, 1957).
11. C. T. Raymo, J. W. Mayer, Trans. IRE vol. NS-8, 157; 1961.
12. H. M. Mann, J. W. Haslett, G. P. Lietz, Trans. IRE vol. NS-8, 151; 1961.
13. A. van der Ziel, Noise, (Prentice Hall, New York, 1954).
14. A. van der Ziel, Fluctuation Phenomena in Semi-Conductors, (Butterworths, London, 1959).
15. F. S. Goulding, W. L. Hansen, Nuclear Instr. and Methods vol. 12, 249; 1961.

16. V. Fano, Phys. Rev. 72, 26; 1947.

17. J. M. Taylor, Semiconductor Particle Detectors, (Butterworths, London, 1963).

18. F. S. Goulding, Lectures given at Herceg-Novi, Yugosl., August, 1965; Lawrence Radiation Laboratory Report, UCRL-16231; 1965.

19. S. O. W. Antman, D. A. Landis, R. H. Pehl, Nuclear Instr. and Methods 40, 272-276; 1966.

20. O. Meyer, H. J. Langmann, Nuclear Instr. and Methods vol. 39, 119-124; 1966.

21. G. Dearnaley, A. B. Whitehead, Nuclear Instr. and Methods 12, 205-226; 1961.

22. N. J. Hansen, Trans. IRE NS-9, 217-233; 1962.

23. G. Dearnaley, J. C. Lewis, Nuclear Instr. and Methods vol. 25, 237-243; 1964.

24. E. D. Klema, Nuclear Instr. and Methods 26, 205; 1964.

25. G. Anderson-Lindström, B. Zausig, Nuclear Instr. and Methods 40, 277-290; 1966.

27. J. L. Blankenship, C. J. Borkowski, Trans IRE vol. NS-8, 17; 1961.

28. Heynes J. R., Hornbeck J. A., Phys Rev., 90, 152; 1953.

29. N. B. Hannay, Semiconductors, (Reinholds, New York, 1961).

30. G. G. George, E. M. Gunnersen, Nuclear Instr. and Methods 25, 253-260; 1964.

31. Strominger, Hollander, Seaborg, Tables of Isotopes, April, 1958, (Berkeley, California).

32. W. Hansen, F. S. Goulding, Proc. Asheville Conference, NAS-NRC Publication 871, 202; 1961.

33. E. Fairstein, Trans. IRE NS-8, 129; 1961.

34. J. W. Mayer, Proc. Asheville Conference, NAS-NRC Publication 871, 3; 1961.

35. W. L. Brown, Trans, IRE NS-8, 2; 1961.

36. G. L. Miller, Proc. Asheville Conference, NAS-NRC Publication 871, 19; 1961.

37. R. W. Klingersmith, Trans IRE vol. NS-8, 112; 1961.

38. R. V. Babcock, Trans IRE vol. NS-8, 98; 1961.

39. J. W. Meyer, Trans. IRE vol. NS-9, 124; 1962.

40. E. Baldinger, W. Czaja, Nuclear Instr. and Methods 10, 237-239; 1961.

41. G. Bemskki, Phys. Rev. 103, 567; 1958.

ACKNOWLEDGEMENTS

The author is indebted to Dr. I. Cooke, for guidance and help during the work. He is very obliged to Professors R. Connor, B. Hogg, F. Kelly, S. Sen and D. Douglas, for their kind loan of most of the equipment used in the experiment and to Mr. F. Konopasek for the assistance in making some of the equipment.

The author is grateful to the staff of the Department of Physics at the University of Belgrade, especially to Professors D. K. Jovanović and A. Milojević, for the leave that enabled him to come to Canada.

Special thanks are due to my friends, L. D. Reed, D. Eaton and G. DeBlonde, for continued encouragement and help during the work.

The author wishes to express his most special thanks to Professor B. G. Whitmore owing to whose kind help he was enabled to come, study and work in the friendly atmosphere of the Department of Physics of the University of Manitoba.